ISTANBUL TECHNICAL UNIVERSITY ★ GRADUATE SCHOOL OF SCIENCE
ENGINEERING AND TECHNOLOGY

INDEX MODULATION-BASED TECHNIQUES FOR DIFFUSIVE MOLECULAR COMMUNICATION SYSTEMS

M.Sc. THESIS

Ahmet ÇELİK

Department of Electronics and Communications Engineering

Telecommunications Engineering Program

JUNE 2019

ISTANBUL TECHNICAL UNIVERSITY ★ GRADUATE SCHOOL OF SCIENCE
ENGINEERING AND TECHNOLOGY

INDEX MODULATION-BASED TECHNIQUES FOR DIFFUSIVE MOLECULAR COMMUNICATION SYSTEMS

M.Sc. THESIS

Ahmet ÇELİK
(504161301)

Department of Electronics and Communications Engineering

Telecommunications Engineering Program

Thesis Advisor: Prof. Dr. Hakan Ali ÇIRPAN
Co-advisor: Assoc. Prof. Ertuğrul BAŞAR

JUNE 2019

**MOLEKÜLER HABERLEŞME SİSTEMLERİ İÇİN
İNDİS MODÜLASYONU TABANLI TEKNİKLER**

YÜKSEK LİSANS TEZİ

Ahmet ÇELİK
(504161301)

Elektronik ve Haberleşme Mühendisliği Ana Bilim Dalı

Telekomünikasyon Mühendisliği Programı

Tez Danışmanı: Prof. Dr. Hakan Ali ÇIRPAN
Eş Danışman: Doç. Dr. Ertuğrul BAŞAR

HAZİRAN 2019

Ahmet ÇELİK, a M.Sc. student of ITU Graduate School of Science Engineering and Technology 504161301, successfully defended the thesis entitled "INDEX MODULATION-BASED TECHNIQUES FOR DIFFUSIVE MOLECULAR COMMUNICATION SYSTEMS", which he prepared after fulfilling the requirements specified in the associated legislations, before the jury whose signatures are below.

Thesis Advisor :	**Prof. Dr. Hakan Ali ÇIRPAN** Istanbul Technical University	....
Co-advisor :	**Assoc. Prof. Ertuğrul BAŞAR** Koç University	....
Jury Members :	**Prof. Dr. İbrahim ALTUNBAŞ** Istanbul Technical University	....
	Assoc. Prof. Ender Mete EKŞİOĞLU Istanbul Technical University	....
	Assoc. Prof. Ali Emre PUSANE Boğaziçi University	....

Date of Submission :   **2 May 2019**
Date of Defense :   **13 June 2019**

FOREWORD

TABLE OF CONTENTS

ABBREVIATIONS

ATD	**:**	Adaptive Threshold Detection
BCSK	**:**	Binary Concentration Shift Keying
BER	**:**	Bit Error Rate
CIR	**:**	Channel Impulse Response
CSK	**:**	Concentration Shift Keying
FTD	**:**	Fixed Threshold Detection
ILI	**:**	Inter-Link Interference
IM	**:**	Index Modulation
ISI	**:**	Inter-Symbol Interference
MC	**:**	Molecular Communication
MCD	**:**	Maximum Count Detector
MCvD	**:**	Molecular Communication via Diffusion
MIMO	**:**	Multiple-Input Multiple-Output
MMs	**:**	Messenger Molecules
MoSK	**:**	Molecule Shift Keying
MSSK	**:**	Molecular Space Shift Keying
PPM	**:**	Pulse Position Modulation
RX	**:**	Receiver
SER	**:**	Symbol Error Rate
SID	**:**	Signal to Interference Difference
SISO	**:**	Single-Input Single-Output
SM	**:**	Spatial Modulation
SMUX	**:**	Spatial Multiplexing
TX	**:**	Transmitter
UCA	**:**	Uniform Circular Array

SYMBOLS

D	: Diffusion Coefficient
$\mathbf{d_{TX\text{-}RX}}$	: Distance between TX Unit and RX Unit
$\mathbf{h_{i,j}[k]}$	: k^{th} Channel Coefficient between TX_i and RX_j
L	: Channel Memory
M	: Number of Molecules
$\mathbf{n_{TX}}$	: Number of TX Antennas
$\mathbf{n_{RX}}$	: Number of RX Antennas
$\mathbf{r_0}$	: Distance between TX and the Center of RX in SISO channel
$\mathbf{R_j[n]}$	: Number of Received Molecules at RX_j at the nth Time Slot
$\mathbf{r_r}$	: Radius of Receiver Antenna
$\mathbf{r[n]}$	: Arrival Vector at the nth Time Slot
$\mathbf{r_{UCA}}$	: Radius of UCA
$\mathbf{RX_j}$	: j^{th} RX Antenna
$\mathbf{s_i[n]}$	: Number of Transmitted Molecules from TX_i at the nth Time Slot
$\mathbf{t_b}$	: Bit Duration
$\mathbf{t_s}$	: Symbol Duration
$\mathbf{TX_i}$	: i^{th} TX Antenna
$\mathbf{v_j}$	: Diversity Combining Vector for RX_j
$\mathbf{x[n]}$	: Input Symbol at the nth Time Slot
$\alpha_{\mathbf{space}}$	: Space Equalization Coefficient
$\alpha_{\mathbf{time}}$	: Time Equalization Coefficient
θ	: Angular Difference between TX Unit and RX Unit

LIST OF TABLES

LIST OF FIGURES

INDEX MODULATION-BASED TECHNIQUES FOR DIFFUSIVE MOLECULAR COMMUNICATION SYSTEMS

SUMMARY

Molecular communication, which is inspired from nature, is a communication technique that enables the data transmission between nano-machines. In the future, nano-machines will be used in many application areas such as bio-medicine, industry, military, however, they will be able to operate only simple tasks individually because of their limited processing power. In order to accomplish complex tasks, nano-machines have to work together and form a nano-network. Molecular communication is a very promising technique to be deployed in nano-networks.

A molecular communication system consists of a transmitter (TX) unit, a receiver (RX) unit and the molecular channel. TX encodes the information on the physical properties of molecules and emits to the channel. RX absorbs the molecules, which propagate in the channel and reach to the surface of RX, and decides to the information. According to the propagation of molecules, there are several kinds of molecular communication forms in the literature. As an example, molecules can be carried by molecular motors or emitted to the channel and directed with the flow. In molecular communication via diffusion (MCvD), molecules are emitted to the liquid environment without drift and propagate with free diffusion. In this thesis, all our works are related with the MCvD.

In single-input single-output (SISO) molecular communication channels, one TX antenna and one RX antenna are used. Information can be encoded on the number of molecules, type of the molecules or release time of molecules etc. Since the diffusion motion of molecules is random in three dimensions of space, there is a probability that a molecule may arrive at the RX late or may never arrive at the RX. The late reaching molecules cause inter-symbol interference (ISI) in the channel.

Multiple-input multiple-output (MIMO) systems have multiple TX and RX antennas. Because of the diffusion, a molecule may reach to the any RX antenna in the channel. In addition to ISI, molecules reach to the unintended RX antenna cause inter-link interference (ILI). In MIMO systems, multiple antennas provide great flexibility. Spatial multiplexing divides the input data and sends each stream from another TX antenna simultaneously. This technique increases throughput but suffers from high ILI since all TX antennas are active at a time. In molecular MIMO systems, spatial codes are also proposed. Nevertheless, molecular communication is disadvantageous for space-time block codes because there are no negative or complex numbers of molecules. Index modulation (IM), in which the information is encoded on TX antenna index, is an effective MIMO technique for MCvD channels. At the TX unit, only one TX antenna is active at a time and the RX unit decodes the data according to the antenna index with the maximum arrival count. In addition, spatial modulation (SM) is an IM-based modulation technique that the information can be encoded on both antenna index and the physical properties of molecules.

In this thesis, two novel methods are proposed for IM-based molecular modulation schemes. Firstly, a novel space-time equalization technique is developed for increasing the error performance of the system. Secondly, a low complexity solution is presented for a possible angular misalignment in the system.

Space-time equalization technique applies an equalization operation to the received signal before demodulation. In space equalization, arrival count of RX antenna's neighbors are multiplied with a coefficient and added to the count of RX antenna. In our studies, this coefficient is found as a positive number so space equalization regains the transmit power and gets effective against ILI. In time equalization, arrival count of RX antenna in the previous time slot is multiplied with a coefficient and added to the count of current time slot. By selecting a negative number as a coefficient, late reaching molecules are removed from the signal and ISI is reduced. Space-time equalization applies both space equalization and time equalization simultaneously for being effective against ISI and ILI at the same time.

Bit error rate (BER) performance of equalization techniques are compared with Monte Carlo simulations. For different system parameters, MCvD channel may be dominated by ISI or ILI. It has been observed that the space equalization technique performs better than time equalization in terms of BER when the channel is dominated by ILI. On the other hand, time equalization is effective for improving error performance in the ISI dominated channels. When compared with the cases without equalization, our findings reveal that both time equalization and space equalization lower the error rate. Moreover, space-time equalization technique reduces ISI and ILI at the same time and increases the error performance of the system significantly.

Second concept proposed in the thesis is a technique that aims to protect the performance of the system against possible misalignment of the system. In the literature, IM-based modulation schemes assume the perfect alignment of TX unit and RX unit. But in MCvD systems, a potential misalignment is possible since TX and RX units are in liquid environment. Against this misalignment case, a low complexity diversity combining method is proposed. At the RX unit, an arrival count vector is generated after the arrival of molecules in each RX antenna is counted. This vector is multiplied with a diversity combining vector to calculate the count of first RX antenna. Cyclic shift of the same diversity combining vector is used to calculate the count of other RX antennas. Finally, calculated counts are compared for deciding to the bit sequence. In our studies, channel impulse response (CIR) in the first time slot is selected as diversity combining vector assuming the availability of CIR at the RX unit.

Symbol error rate (SER) performance of the diversity combining method is investigated with Monte Carlo simulations. As the angular misalignment between TX unit and RX unit in the yz plane increases, error rate of the conventional method also increases. When RX antenna is aligned to the middle of two neighboring TX antennas, which is the worst case, bit sequence can not be decoded. Proposed diversity combining method protects the system for angular misalignment and even in the worst case a desirable error rate is obtained. In ILI dominated channels, proposed method performs better than conventional method for both misaligned channels or perfectly aligned channel. When ISI dominates the channel, our proposed method yields a worse error performance than conventional method in perfectly aligned channel. Still, protection of diversity combining against the misalignment of the system makes our proposed method an effective and low complexity technique.

MOLEKÜLER HABERLEŞME SİSTEMLERİ İÇİN İNDİS MODÜLASYONU TABANLI TEKNİKLER

ÖZET

Moleküler haberleşme, nano makineler arasındaki haberleşmeyi sağlamak amacı ile doğadan esinlenilerek ortaya çıkmış bir haberleşme tekniğidir. Nano makineler gelişen teknoloji ile birlikte gelecekte tıp, sanayi, askeri gibi uygulama alanlarında kullanılacaktır ancak işlemci kapasitelerinden dolayı nano boyutlarındaki bu cihazlar tek başlarına sadece basit işlemleri gerçekleştirebileceklerdir. Karmaşık görevleri başarabilmek için koordineli olarak çalışarak bir nano ağ oluşturmaları gerekmektedir. Moleküler haberleşme nano ağlarda kullanılmak için en ümit verici haberleşme tekniğidir.

Moleküler haberleşme sistemleri alıcı ünitesi, verici ünitesi ve kanaldan oluşur. Verici, bilgiyi moleküllerin fiziksel özelliklerine kodlayarak kanala gönderir. Kanalda hareket eden moleküllerin alıcıya ulaşması ile alıcıda moleküller sayılır ve bilgiye karar verilir. Moleküllerin taşınmasına göre literatürde çeşitli moleküler haberleşme teknikleri bulunmaktadır. Moleküler motorlar kullanılarak mikrotübüller üzerinden moleküller taşınabildiği gibi moleküllerin sıvı ortama bırakılarak bir akıntı ile yönlendirilmesi de mümkündür. Difüzyon aracılığıyla moleküler haberleşme yönteminde ise moleküller hareketsiz sıvı ortama bırakılır ve tamamen serbest difüzyon ile hareket eder. Bu tezdeki bütün çalışmalar difüzyon aracılığı ile moleküler haberleşme üzerine yapılmıştır.

Tek-girişli tek-çıkışlı (SISO) moleküler haberleşme sistemlerinde bir alıcı ve bir verici anteni bulunur. Bilgi, moleküllerin yoğunluk, cins, serbest bırakılma anı gibi fiziksel özelliklerine kodlanır. Moleküllerin difüzyon hareketi üç uzaysal boyutta tamamen rastgele olduğu için kanala gönderilen moleküllerin alıcıya geç ulaşma veya hiç ulaşmama ihtimali bulunmaktadır. Geç ulaşan moleküller, daha sembollerde bozucu etkiye sebep olacağından dolayı semboller arası girişim oluşturur.

Çok-girişli çok-çıkışlı (MIMO) moleküler haberleşme sistemlerinde ise birden fazla alıcı ve verici antenleri bulunur. Moleküllerin rastgele hareketinden dolayı kanala gönderilen bir molekülün herhangi bir alıcı antene ulaşma olasılığı bulunmaktadır. Bu sebeple MIMO sistemlerde semboller arası girişime ek olarak moleküllerin istenmeyen alıcıya ulaşmayı sonucu ortaya çıkan kanallar arası girişim de dikkate alınmalıdır. Sistem parametrelerine göre kanalda semboller arası girişim veya kanallar arası girişim baskın olabilmektedir. Örneğin sembol süresi arttıkça, ilk sembol aralığında daha fazla molekül iletileceği için semboller arası girişim azalır ancak diğer antenlerde alınan moleküller de artacağı için kanallar arası girişim artar. Alıcı ve verici ünitelerinde antenlerin daha ayrık konumlandırılmaları kanallar arası girişimi azaltacaktır. Ancak komşu alıcı antenler kanaldaki molekülleri soğurduğu için moleküllerin daha geç varmasını engeller. Bu durumda antenlerin birbirlerine yaklaştırılmaları da semboller arası girişimi azaltacaktır.

MIMO sistemler birden fazla anten bulunması ile önemli esneklikler sağlar. Uzaysal çoğullama ile giriş bilgi dizisi bölünerek aynı anda farklı verici antenlerden gönderilebilir ve böylece iletişim hızı arttırılabilir ancak uzaysal çoğullama aynı anda bütün vericilerin aktif olması sebebiyle kanallar arası girişimden yüksek derecede etkilenir. Moleküler haberleşme kanalında Alamouti kodundan esinlenilerek uzay-zaman blok kodları da denenmiştir ancak negatif veya karmaşık sayıda molekül olmadığı için başarılı olmamıştır.

İndis modülasyonu, MIMO sistemlerde verici antenin indisine bilginin kodlandığı etkili bir modülasyon tekniğidir. Radyo frekansı haberleşme sistemlerinden esinlenilerek moleküler haberleşme sistemleri için tasarlanan indis modülasyonu şemalarında verici tarafında aynı anda sadece bilgi sembolüne karşılık gelen anten aktiftir. Alıcı tarafında ise en yüksek sayı kod çözücüsü düşük karmaşıklıklı bir kod çözücü olarak önerilmiştir ve en yüksek sayıda molekülün alındığı anten indisine bilgi sembolü olarak karar verir. Ek olarak, moleküler haberleşme literatürüne indis modülasyonu tabanlı bir teknik olan uzaysal modülasyon şemaları önerilmiştir. Uzaysal modülasyonda bilgi hem anten indisine hem de moleküllerin fiziksel özelliklerine kodlanır. Molekül yoğunluğu, molekül tipi, molekülün kanala gönderilme anı gibi fiziksel özellikler bilgi taşımak amacı ile kullanılabilir.

Bu tezde, indis tabanlı modülasyon şemalarına yönelik iki özgün yöntem önerilmiştir. Öncelikle, sistemin hata performansını arttırmak amacı ile uzay-zamanda eşitleme tekniği geliştirilmiştir. İkinci olarak da kanal modelinde oluşabilecek hizalanma sorunlarına karşı sistemin performansını toparlayacak düşük karmaşıklıklı bir yöntem paylaşılmıştır.

Uzay-zamanda eşitleme yönteminde alınan sembol çözülürken aynı zaman aralığında komşu antenlerde alınan molekül sayıları ve bir önceki zaman aralığında aynı antende alınan molekül sayıları da hesaba katılır. Sadece komşu antenlerin işleme alındığı uzay eşitleme yönteminde bir antenin komşularındaki molekül sayısı bir katsayı ile çarpılarak o antendeki molekül sayısına eklenir ve elde edilen molekül sayıları karşılaştırılarak bilgi dizisine karar verilir. Yapılan çalışmalarda bu katsayının çoğunlukla pozitif olduğu belirlenmiştir yani uzayda eşitleme kanalda kaybettiği gücü yeniden kazanarak kanallar arası girişime karşı etkili olmayı hedefler. Zamanda eşitleme tekniğinde antenin bir önceki zaman aralığında aldığı molekül sayısı bir katsayı ile çarpılarak molekül sayısına eklenir. Bu katsayının da negatif olması kanala gönderildikten sonra alıcıya geç ulaşan moleküllerin hesaptan çıkarılmasını yani semboller arası girişimin azaltılmasını sağlar. Uzay-zamanda eşitleme tekniğinde ise hem uzay hem de zamanda eşitleme aynı anda kullanılarak tekniklerin performansı arttırılır.

Monte Carlo simülasyonları yapılarak uzay-zamanda eşitleme yöntemlerinin bit hata performansları karşılaştırılmıştır. Uzayda eşitleme yöntemi kanallar arası girişimin baskın olduğu durumlarda zamanda eşitlemeden daha iyi hata performansı gösterirken semboller arası girişimin baskın olduğu kanallarda zamanda eşitleme etkin olmuştur. Bu durumun açıklaması olarak uzayda eşitlemenin kanallar arası girişime karşı, zamanda eşitlemenin ise semboller arası girişime karşı etkili olması gösterilebilir. Eşitleme olmayan durumlarla karşılaştırıldığında bu iki teknik de hata oranını düşürmüştür. Bu iki tekniğin eş zamanlı olarak kullanıldığı uzay-zamanda eşitleme tekniği ise hem kanallar arası girişim hem de semboller arası girişimi azaltarak sistemin hata performansını ciddi ölçüde geliştirmiştir.

Tezde önerilen ikinci yaklaşım moleküler haberleşme kanallarındaki olası hizalanma hatalarına karşı performansı korumayı hedefleyen bir tekniktir. Literatürde indis modülasyonu uygulanan sistemlerde alıcı ve verici ünitelerin karşılıklı olduğu ve haberleşme süresince mükemmel hizalanmanın korunduğu kabul edilmiştir. Ancak moleküler haberleşme sistemi sıvı ortamda olduğu için hizalanma hatalarının olması mümkündür. Bu duruma karşılık düşük karmaşıklıklı çeşitleme birleştiricisi yöntemi önerilmiştir. Alıcıda moleküller sayıldıktan sonra elemanları her antendeki molekül sayıları olan bir alınan molekül vektörü oluşturulur. Bu vektör çeşitleme birleştirme vektörü ile çarpılarak ilk antendeki molekül sayısı yeniden hesaplanır. Birinci antenden kaç yan antene bakıldığına göre aynı çeşitleme birleştirme vektörünün o kadar döngüsel ötelenmişi kullanılarak her antendeki molekül sayısı hesaplanır ve yeni hesaplanan molekül sayılarına göre bilgi dizisi en yüksek sayı kod çözücüsü ile çözülür. Tezdeki çalışmalarımızda kanal dürtü yanıtının alıcıda hesaplanabildiği varsayılarak çeşitleme birleştirme vektörü kanal dürtü yanıtının ilk zaman aralığındaki değerleri olarak seçilmiştir.

Çeşitleme birleştiricisi yönteminin performansı Monte Carlo simülasyonları ile incelenmiştir. Alıcı ve verici arasında *yz* düzleminde açısal olarak fark oluşmaya başladıkça geleneksel yöntemin hata oranı artmaya başlamıştır. Alıcı, komşu vericilerinin orta noktasına gelecek şekilde hizalandığında yani en kötü senaryoda bilgi dizisi çözülememiştir. Önerilen yöntem ise açısal kaymalara karşı etkili bir koruma oluşturmuştur ve en kötü durumda bile kabul edilebilir hata performansı göstermiştir. Kanallar arası girişimin baskın olduğu sistemlerde önerilen yöntem, geleneksel yöntemden mükemmel hizalanma durumunda bile daha iyi sonuç vermiştir. Semboller arası girişimin baskın olduğu mükemmel hizalanmış kanallarda ise önerilen yöntem, geleneksel yöntemin gerisinde kalmıştır ancak olası açı kaymalarında gösterdiği performans koruması sebebiyle çeşitleme birleştiricisi yöntemi düşük karmaşıklıklı ve güçlü bir teknik olmuştur.

1. INTRODUCTION

1.1 Nanonetworks and Molecular Communication

Nanonetworks, collaboration of nano-machines working together, have a great potential in many areas such as biomedicine, industry, military and environment for the future [1]. With the advancements in nanotechnology, it will be possible for human made nano devices to be inside our body in order to support immune system, monitor health status, deliver drugs to destination etc. The operating area of nano-machines will not be limited with the human body. Controlling quality of food, detecting chemical attacks, reducing air pollution and cleaning waste water are some other important tasks that nano-machines will accomplish.

A nano-machine is the main operative element of the nanonetworks. Due to their small sizes which can vary from one to a hundred nanometers, they can only execute simple jobs individually [2]. Sensing, actuating, computing and storing data are examples that nano-machines can perform with their nanoscale components: sensors, actuators, processing unit, storage unit. The low complexity processor of nano-machines is another factor that limits them for a complex operation [1]. To overcome this limitation, communication is an essential feature for nano-machines. By communicating with each other while each of them performing its own task, nano-machines form a nanonetwork and as a result of this teamwork, much more complicated jobs can be handled effectively.

In nano scale, traditional communication techniques have some disadvantages. Radio frequency communication uses electromagnetic waves to exchange information and have a requirement that antenna length condition which is proportional with the wavelength of the signal must be provided. To radiate from an antenna in nanometer scales, very high frequency modulators should be developed for nano-machines which is very challenging [1, 3]. In optical communication, where the light is used as a

data carrier, the necessity of a waveguide or line of sight makes it inapplicable for nanonetworks [3]. Carrying information with ultrasonic waves is another method for communication, named as acoustic communication. Due to the size of transducers, which are used for sensing pressure variations to decode the data from ultrasonic waves, implementing acoustic communication on nano-machines is also unsuitable [1].

Molecular communication (MC), a bio-inspired technique, is a promising solution for nanonetworks. Motivated from intracellular, intercellular and inter-organ communications in nature, chemical signals are used for data transmission in MC [4]. The MC system consists of transmitter nano-machine, receiver nano-machine and the channel. At the transmitter nano-machine, information is encoded into molecules and released to the channel where molecules can propagate such as liquid or gaseous environment. Receiver nano-machine detects the molecules that reach to its sensors or receptors and decodes the data [5].

According to the transmission of molecules, MC can be classified in three categories: walkway-based, flow-based and diffusion-based [2]. In walkway-based MC, there is a direct path between the transmitter nano-machine and the receiver nano-machine. Using molecular motors is the most common research topic for walkway-based MC where the molecules are carried with molecular motors along the microtubules [6]. In flow-based MC, while molecules are propagating with diffusion, a flow is assisted to the molecules in order to increase the speed of propagation and transmit longer distances. Motion of hormones in blood is an inspiring example of flow-based communication from the nature. In diffusion-based MC, molecules which are released from transmitter move randomly in channel with free diffusion. As there are no additional sources, it is a slower type of communication compared to flow-based MC [3]. Diffusion-based MC is also known as molecular communication via diffusion (MCvD) and all our work relies on MCvD. From this point of thesis, molecular communication will refer to the MCvD, transmission of molecules in free diffusion channel.

1.2 Molecular Communication via Diffusion

MCvD is a type of molecular communication in which molecules propagate in a liquid environment with free diffusion. Due to the nature of diffusion, molecules

move randomly in both directions, named as Brownian motion and this motion of molecules is modeled with random-walk process [4]. After the release of molecules to the channel, some of the molecules will reach to the receiver nano-machine in the intended time slot while others continue to their random movement. In addition, a part of the molecules will arrive late at the receiver nano-machine which will lead to inter-symbol interference (ISI) [7].

Data transmission in single-input single-output (SISO) MCvD systems is ensured by encoding the information on the physical properties of the molecules such as concentration, type, time of release etc. [8–11]. As an example of carrying data with concentration, each symbol can be represented with different number of molecules. After the transmission, data is demodulated at the receiver nano-machine by counting the number of received molecules and comparing with the threshold levels. On the other hand, different types of molecules can be used for different symbols and at the receiver nano-machine, molecule type with the maximum number is decided as the received symbol.

Multiple-input multiple-output (MIMO) systems, using multiple antennas in both transmitter and receiver side, is an interesting frontier for MCvD channels in order to achieve higher data rates and better error performance. In diffusive MIMO systems, inter-link interference (ILI) should be taken into account in addition to ISI. As there are multiple receiver antennas, molecules which are absorbed in unintended receiver result in ILI. [12, 13] consider to divide input data into parallel streams and send from different transmit antennas. By multiplexing data in spatial domain, this technique combats with ISI well, but suffers from high ILI as all the transmitters are active at the same time. In [14], two spatial codes, Alamouti-type coding and repetition MIMO coding, are introduced for 2x2 MIMO diffusion channel. It has been demonstrated that repetition code, which sends same data symbol from both antennas in the same time slot, has a better error performance compared to Alamouti-type coding.

Index modulation (IM) is a popular MIMO technique in radio frequency communication [15, 16]. IM scheme uses antenna indices as a source of information. IM-based techniques are studied recently in molecular communication. [17] proposes a novel IM-based modulation scheme which combats with interference effectively. Also, encoding the data in both transmitter antenna index and the physical property

3

of molecules such as type, concentration level and pulse position is proposed to the literature [17–19].

1.3 Problem Statement and Contribution of Thesis

MIMO techniques are essential for molecular communication channels in order to provide high speed data transmission. However, in MIMO systems, random movement of molecules results in both ISI and ILI. A novel space-time equalization technique is proposed for IM-based modulation schemes in molecular MIMO systems to reduce error rate and improve performance. After the arrival of molecules at the receiver nano-machine, this technique is applied as a preliminary step of demodulation. Using only space domain, only time domain or both space and time domain are possible options.

In space equalization, a linear operation is applied between the selected receiver and its neighboring receivers. Here, linear operation is multiplying the molecule count in the neighbors with a coefficient and adding to the selected receiver. The aim of space equalization is reducing the effect of ILI by using the molecules which arrived in neighboring receivers unintentionally. In time equalization, linear operation is applied in a similar way, but between the current time slot and the previous time slot of the selected receiver. With the time equalization, reducing the effect of ISI is aimed. By combining the space equalization and the time equalization, space-time equalization comes up which aims ISI and ILI simultaneously and improves error performance significantly.

IM-based modulation schemes in the literature assumes that corresponding transmitters and receivers are perfectly aligned to each other. Since nano-machines are located in a liquid environment, losing the alignment in practical scenarios is possible with the movement of nano-machines. A low-complexity technique is proposed in order to provide robustness against the angular misalignment. At the receiver nano-machine, received molecule vector is multiplied with a linear diversity combiner in this technique and the resulting vector is demodulated. Heuristically, diversity combiner vector is selected as the first column of channel coefficient matrix which is the channel impulse response in the first time slot.

4

1.4 Outline

The outline of the thesis is as follows:

In Chapter 2, a brief overview on the motion of molecules, MCvD channel models, SISO and MIMO modulation techniques in the existing literature are given. Chapter 3 describes the space equalization, time equalization and space-time equalization techniques in details. In Chapter 4, a low complexity solution for IM-based modulation schemes in a molecular MIMO channel with angular misalignment is introduced. Simulation results are presented and the numerical results are discussed in chapter 5. Finally, conclusion is made in chapter 6.

2. MOLECULAR COMMUNICATION VIA DIFFUSION

In MCvD, propagation of molecules between the transmitter (TX) and the receiver (RX) is provided with free diffusion without drift. This section starts with explaining diffusion behaviour of molecules. Afterwards, MIMO channel model is presented since our works rely on MIMO techniques but before that, a basic SISO model is given to have a good understanding on diffusion channel by deriving hitting probabilities and channel coefficients. Lastly, some modulation techniques in the literature are mentioned.

2.1 Diffusion Channel and System Model

2.1.1 Behaviour of molecules in diffusion environment

The diffusion of molecules in an aqueous environment is named as Brownian motion. While propagating in a homogeneous medium without any additional sources or flow, molecules move randomly in both three spatial dimensions [4]. Since no energy is used to direct molecules, free diffusion is a slow type of communication but it has an advantage in power consumption.

The process of Brownian motion, also known as random-walk, is described in [3]. By dividing time into discrete steps, ΔT, location of the molecule at time $t = i\Delta T$ can be found as

$$(x_i, y_i, z_i) = (x_{i-1}, y_{i-1}, z_{i-1}) + (\Delta X, \Delta Y, \Delta Z)$$
$$i = 1, 2, \ldots, k \tag{2.1a}$$

$$\Delta X \sim \mathcal{N}(0, 2D\Delta T), \tag{2.1b}$$

$$\Delta Y \sim \mathcal{N}(0, 2D\Delta T), \tag{2.1c}$$

$$\Delta Z \sim \mathcal{N}(0, 2D\Delta T), \tag{2.1d}$$

where (x_0, y_0, z_0) is the initial position of the molecule, $(\Delta X, \Delta Y, \Delta Z)$ is the displacement of the molecule, $\mathcal{N}(0, 2D\Delta T)$ is a normal random variable with mean 0

and variance $2\Delta T$. Since molecules propagate with free diffusion in medium, means of the displacement random variables in both three dimension are zero. Also, D is the diffusion coefficient of molecules and dependent with the viscosity of the liquid, temperature of the medium and the radius of the molecule.

2.1.2 SISO system model

SISO system model consists of a single TX and a single RX in the channel where molecules propagate with free diffusion. TX is a point source and releases messenger molecules (MMs) to the liquid environment. RX is in a spherical shape with radius r_r and absorbs MMs from the channel. System model with one point source and one spherical receiver can be seen in Fig. 2.1. Here, r_0 denotes the distance between the point source and the center of the RX.
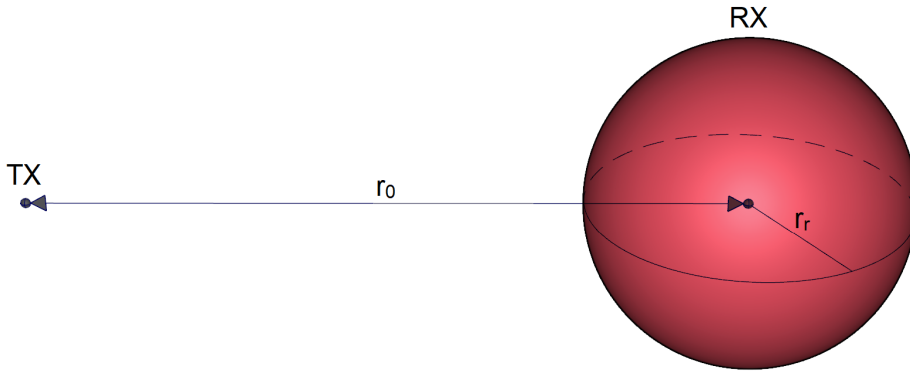
Figure 2.1 : SISO channel model.

TX emits MMs to the medium and MMs starts to move in the diffusion channel until it is absorbed by a RX. Using Fick's diffusion equation and boundary conditions, [20] derives the channel impulse response (CIR) for MMs. Hitting rate of MMs with respect to time is

$$f_{hit}(t) = \frac{r_r}{r_0} \frac{1}{\sqrt{4\pi Dt}} \frac{r_0 - r_r}{t} e^{-\frac{(r_0 - r_r)^2}{4Dt}}. \tag{2.2}$$

By integrating $f_{hit}(t)$, cumulative distribution function of MMs' hitting probability until t is

$$F_{hit}(t) = \frac{r_r}{r_0} \text{erfc}\left[\frac{r_0 - r_r}{\sqrt{4Dt}}\right]. \tag{2.3}$$

The two formulas, (2.2) and (2.3), are important to characterize the diffusion channel. In Fig. 2.2, hitting rate of the MMs can be seen for the values of $r_r = 5\mu m$, $r_0 = 12\mu m$, $D = 79.4\mu m^2/s$. Hitting rate increases fast at start and after a peak value, it decreases by time. As a result of Brownian motion, it is possible for a molecule to travel in the channel for a long time and reach to the RX. Also, it can be calculated that the cdf of hitting probabilities converges to $\frac{r_r}{r_0}$ as time goes to infinity. So, it is not expected to absorb all the molecules which are emitted from the TX.
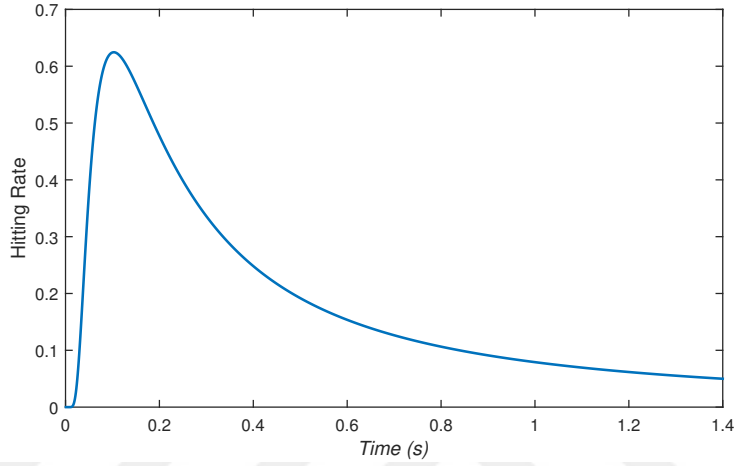
Figure 2.2 : Hitting rate of MMs in SISO channel.

Communication is ensured by sending symbols in consecutive time slots. The probability of a molecule reaching to a RX in the kth time slot is defined as k^{th} channel coefficient, $h[k]$. Channel coefficients can be calculated as

$$h[k] = F_{hit}(kt_s) - F_{hit}((k-1)t_s)$$
$$k = 1, 2, \ldots, L$$

(2.4)

where L is the channel memory and t_s is the symbol duration. Theoretically, channel coefficient vector has infinite number of elements. But for practical purposes, first L coefficients can be used for simulating the channel model effectively [21].

The channel coefficient in the first time slot, $h[1]$, is the intended symbol of communication while $h[k]$, $k \geq 2$ represents the late-reaching molecules which cause ISI in the channel. There is a trade-off between the data rate and ISI effect which are directly related with t_s. Let b be the bits per symbol, bit duration t_b can be calculated as $t_b = \frac{t_s}{b}$ and data rate is the multiplicative inverse of bit duration. As t_s decreases, molecules are released more often and data rate increases but $h[1]$ also decreases which results with high ISI. Since it is not possible to eliminate the ISI effect completely, t_s

9

should be decided for the condition that channel coefficients are ordered from high to low ($h[1] > h[2] > h[3] \ldots$).

Let s^{TX} be the number of molecules emitted from the TX. Since channel coefficients are the hitting probabilities, number of received molecules in the nth time slot is

$$R_{single\ emission}[n] \sim \mathscr{B}\left(s^{TX}, h[n]\right), \tag{2.5}$$

where $\mathscr{B}(n, p)$ is a Binomial random variable with parameters n and p. This formula is valid for only one emission of TX. But for communication, TX continues to emit molecules in the consecutive time slots. So, number of received molecules should be modified as

$$R[n] \sim \begin{cases} \sum\limits_{k=1}^{n} \mathscr{B}\left(s[k], h[n-k+1]\right), & \text{if } n < L, \\ \sum\limits_{k=n-L+1}^{n} \mathscr{B}\left(s[k], h[n-k+1]\right), & \text{if } n \geq L, \end{cases} \tag{2.6}$$

where $s[k]$ denotes the number of transmitted molecules at the kth time slot. Binomial random variables can be approximated to normal random variables by $\mathscr{B}(n, p) \sim \mathscr{N}(np, np(1-p))$. As also derived in [22], arrival count at the nth time slot can be shown as $R[n] \sim \mathscr{N}\left(\mu[n], \sigma^2[n]\right)$ where

$$\mu[n] = \sum_{k=n-L+1}^{n} s[k]h[n-k+1] \tag{2.7}$$

and

$$\sigma^2[n] = \sum_{k=n-L+1}^{n} s[k]h[n-k+1]\left(1-(h[n-k+1])\right). \tag{2.8}$$

Note that, TX and RX must be synchronized in time to derive arrival model presented in this section. As explained in [23], synchronization between TX and RX can be provided.

2.1.3 MIMO system model

MIMO molecular communication channel consists of a single TX unit and a single RX units which are equipped with multiple TX and RX antennas on them. The body of TX unit is transparent to MMs and has n_{TX} transmit antennas which emit MMs independently. RX unit has a reflecting surface and has n_{RX} spherical absorbing antennas with radius r_r. TX_i and RX_j refer to the ith TX antenna and the jth RX antenna

10

throughout the paper where $i \in (1, 2, \ldots, n_{TX})$ and $j \in (1, 2, \ldots, n_{RX})$. In literature, there are different approaches in placing TX and RX antennas to their corresponding TX unit and RX unit. [13, 14] prefer a linear formation while [17, 19] prefer a uniform circular array (UCA) formation which we refer as linear MIMO model and UCA MIMO model respectively.

To begin with the linear MIMO model which is presented in Fig. 2.3, the distance between the TX unit and the RX unit is denoted by d_{TX-RX}. The centers of neighboring RX antennas are separated with distance d_z, so as the distance between neighboring TX antennas. The centers of RX antennas are aligned to the corresponding TX antennas perfectly so that the minimum distance between the TX_i and RX_i can be calculated as $d_{TX-RX} - 2r_r$.

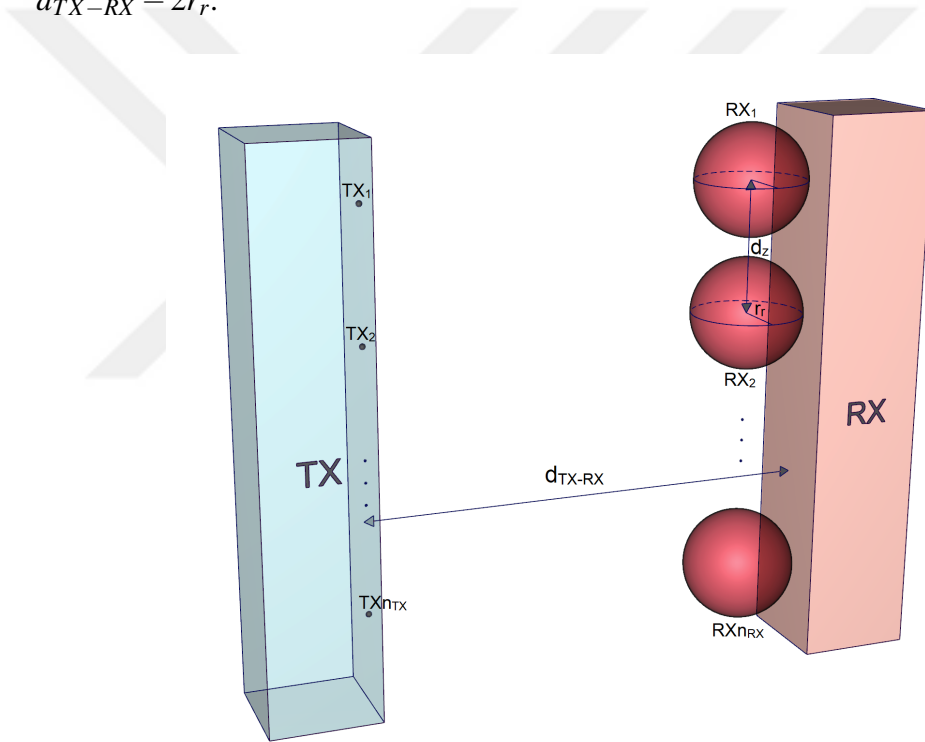**Figure 2.3** : Linear MIMO channel model.

There are no closed form equations for deriving channel coefficients in MIMO channels yet. In literature, Brownian motion-based Monte Carlo simulations [13, 17] or machine learning algorithms [24] are used for calculating hitting rate distributions, $F_{ij}(t)$. Here, $F_{ij}(t)$ denotes the probability of a molecule emitted from TX_i to reach RX_j until time t.

By taking derivative of $F_{ij}(t)$, the pdf of channel response, $f_{ij}(t)$ can be found which is presented in Fig. 2.4 for 2x2 linear MIMO model. This figure is generated with Monte Carlo simulations for the parameters $r_r = 5\mu m$, $d_{TX-RX} = 20\mu m$, $d_z = 12\mu m$, $D = 79.4\mu m^2/s$. Here, $f_{11}(t)$ denotes the hitting rate between TX_1 and RX_1, $f_{12}(t)$ denotes the hitting rate between TX_1 and RX_2. Since 2x2 linear MIMO channel is symmetrical, $f_{11}(t)$ is equal to $f_{22}(t)$ and $f_{12}(t)$ is equal to $f_{21}(t)$. In molecular MIMO channels, molecule emitted from TX_i is desired to be absorbed at RX_i but can be absorbed in one of all RX antennas because of the random movement of molecules. For $(i \neq j)$, $f_{ij}(t)$ shows the molecules that received in the unintended RX antennas which causes ILI in the system. In addition, $f_{SISO}(t)$ shows the hitting rate between TX_1 and RX_1 if there was no other RX antenna in the channel. As it is seen in the figure, $f_{11}(t)$ is smaller than $f_{SISO}(t)$ because neighboring RX antenna absorbs the molecules which reach to its surface.
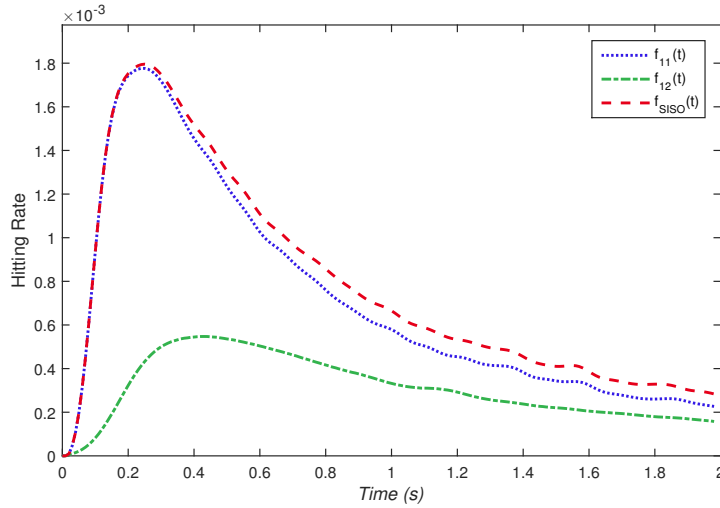
Figure 2.4 : Hitting rate of MMs in MIMO channel.

In UCA MIMO model, which can be seen in Fig. 2.5, RX and TX antennas are placed angular-wise separated from each other, forming a uniform circle. Here, d_{TX-RX} denotes the distance between TX and RX units and r_{UCA} denotes the radius of UCA. Since RX antennas are spherical in shape, centers of RX antennas form a UCA with r_{UCA}. Thus, the closest distance between the center of UCA and the projection of RX antenna to the surface of RX unit is $r_{UCA} - r_r$. Similar to linear MIMO model, TX and RX antennas are perfectly aligned and the closest distance between corresponding TX and RX antennas is $d_{TX-RX} - 2r_r$.

12
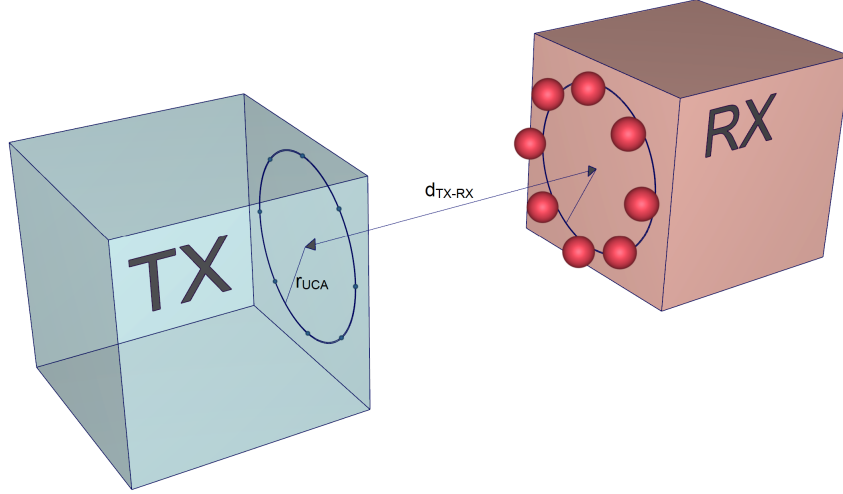
Figure 2.5 : UCA MIMO channel model.

In our work, hitting rate distributions are obtained by Monte Carlo simulations. Channel coefficients can be calculated as

$$h_{i,j}[k] = F_{ij}(kt_s) - F_{ij}((k-1)t_s), \tag{2.9}$$

where $h_{i,j}[k]$ denotes channel coefficient between TX_i and RX_j at the kth time slot. With the channel coefficients, number of molecules at the RX antennas can be found by modeling transmissions as independent Binomial events [17]. Let $s_i[k]$ be the number of molecules emitted from TX_i at the kth time slot, arrival count of RX_j at the nth time slot is $R_j[n] \sim \mathcal{N}\left(\mu_j[n], \sigma_j^2[n]\right)$ where

$$\mu_j[n] = \sum_{k=n-L+1}^{n} \sum_{i=1}^{n_{TX}} s_i[k]h_{i,j}[n-k+1] \tag{2.10}$$

and

$$\sigma_j^2[n] = \sum_{k=n-L+1}^{n} \sum_{i=1}^{n_{TX}} s_i[k]h_{i,j}[n-k+1]\left(1 - (h_{i,j}[n-k+1])\right). \tag{2.11}$$

2.2 SISO Modulation Techniques

In MCvD, modulation techniques use physical properties of molecules as a carrier in SISO systems. Concentration shift keying (CSK), molecular shift keying (MoSK) and pulse position modulation (PPM) are the most popular SISO modulation techniques in the literature.

2.2.1 Concentration shift keying

The amplitude of emitted molecules is the information carrier in CSK, similar to the Amplitude Shift Keying in the radio frequency communications. In order to transmit k bits per symbols, 2^k different concentration levels should be used for corresponding symbols [8]. Binary CSK (BCSK) is the type of CSK where one bits per symbol is transmitted. For bit "1", a certain amount of molecules are transmitted while there are no transmissions for bit "0".

Let M^{CSK} be the number of molecules transmitted for bit "1" in BCSK. If $x[n]$ is denoted as the binary input data, modulated data can be calculated as

$$s[n] = M^{CSK}x[n]. \tag{2.12}$$

At the RX, absorbed molecules are counted and data is demodulated by comparing with pre-defined thresholds, named as fixed threshold detection (FTD). If the symbol carries k bits, there are 2^k concentration levels and $2^k - 1$ threshold levels should be used for deciding bit sequence eventually. For BCSK, one threshold level is needed. If number of received molecules are more than threshold, symbol is decoded as bit "1", otherwise bit "0". FTD operation for BCSK with threshold τ is

$$\hat{x}[n] = \begin{cases} 1, & \text{if } R[n] \geq \tau, \\ 0, & \text{if } R[n] < \tau. \end{cases} \tag{2.13}$$

Adaptive threshold detection (ATD) is another demodulation technique proposed by [25]. In ATD, if more molecules are received than the previous time slot, symbol is decided as bit "1", otherwise bit "0". For decoding BCSK, ATD can be shown as

$$\hat{x}[n] = \begin{cases} 1, & \text{if } R[n] \geq R[n-1], \\ 0, & \text{if } R[n] < R[n-1]. \end{cases} \tag{2.14}$$

2.2.2 Molecular shift keying

The information carrier is the type of molecules in the MoSK. For k bits per symbol, 2^k different type of molecules are needed. Each symbol is represented with a distinct type of molecule and during transmission, only one type of molecule is sent at a time [8]. In Binary MoSK, one bit per symbol is transmitted and two different molecule types are needed which can be shown as

$$s[n] = \begin{cases} M_A, & \text{if } x[n] = 1, \\ M_B, & \text{if } x[n] = 0, \end{cases} \tag{2.15}$$

where M_A and M_B are number of transmitted molecules in type A and type B respectively.

At the RX, different type of molecules are counted separately. For demodulating MoSK, molecule type with the maximum number is decided as the transmitted symbol and the bit sequence is demodulated.

2.2.3 Pulse position modulation

In PPM, information is encoded into the release time of the molecules [11]. In order to transmit k bits per symbol, time slot is divided into 2^k parts and sending molecules to channel at the beginning of each these parts represents a different symbol. For binary PPM, time slot is divided into two pieces. Transmission at the beginning of time slot represents bit "1" while transmission at the middle of time slot represents bit "0".

After the transmission, demodulated signal can be decided by comparing the arrival count with thresholds or finding the time with the maximum molecule absorption at the RX [26].

2.3 MIMO Modulation Techniques

MIMO channels offer great flexibility at both TX and RX units as there are multiple antennas. Spatial multiplexing (SMUX), spacial coding, IM-based modulations are MIMO techniques that are proposed to the molecular communication literature.

2.3.1 Spatial multiplexing

In SMUX, input data is divided into n_{TX} streams and each stream is sent from different TX antenna simultaneously [12]. Transmission vector of SMUX is

$$G_{SMUX} = \begin{bmatrix} s_k & s_{k+1} & \cdots & s_{n_{TX}-k+1} \end{bmatrix}, \tag{2.16}$$

where i^{th} element of the transmission vector represents the symbol transmitted from TX_i in one time slot. At the RX unit, each RX antenna demodulates the received signal independently.

SMUX is successful in combating with ISI. As data is divided intro streams and sent simultaneously, symbol duration increases under the same data rate with SISO modulation techniques. However, SMUX suffers from high ILI since both TX antennas are active at the same time.

2.3.2 Spatial coding

In [14], two spatial diversity techniques, in which the same data can be transmitted multiple times from different TX antennas or in another time slot, are proposed to the literature. Repetition MIMO coding uses both RX antennas for sending the same data. So, the transmission vector can be shown as

$$G_{Repetition} = \begin{bmatrix} s_k & s_k & \cdots & s_k \end{bmatrix}. \tag{2.17}$$

Repetition MIMO coding uses ILI for its own benefit because signal power can be increased by combining received signals since transmitted data in both TX antennas are exactly the same. Secondly, Alamouti-type coding, which is inspired from the Alamouti space-time block coding scheme in the radio frequency communication, uses both time and space domain for spacial diversity. Transmission matrix of Alamouti-type coding for 2x2 MIMO channel is

$$G_{Alamouti} = \begin{bmatrix} s_k & s_{k+1} \\ M - s_{k+1} & s_k \end{bmatrix}. \tag{2.18}$$

In the transmission matrix, columns represent the TX antennas and the rows represent consecutive time slots. As an example, TX_1 emits s_k in the first time slot and the inverse of s_{k+1} in the following time slot. Alamouti-type coding has a poor performance for molecular communication since negative or complex values for number of molecules does not exist.

2.3.3 Index modulation-based techniques

IM-based techniques, which are among the most recent approaches for molecular MIMO, introduce promising results in terms of error performance. These techniques uses TX antenna indices as a source of information.

Molecular space shift keying (MSSK) is an IM-based modulation scheme that the information is only encoded on the TX antenna index. The index of each TX antenna

represents a different MSSK symbol and only one TX antenna can be active at a moment. For n_{TX} antennas, $\log_2 n_{TX}$ bits per symbol is transmitted. The number of molecules emitted from TX_i at the nth time slot can be shown as

$$s_i[n] = \begin{cases} M^{MSSK}, & \text{if } x[n] = i, \\ 0, & \text{otherwise}, \end{cases} \qquad (2.19)$$

where $x[n]$ is the input data and M^{MSSK} is the number of molecules transmitted in one time slot. At the RX unit, absorbed molecules are counted and the RX antenna index with the maximum number of molecules is decided as the output data. This demodulation method is named as maximum count detector (MCD) and can be shown as

$$\hat{x}[n] = \arg \max_{j \in [1, \cdots, n_{RX}]} R_j[n]. \qquad (2.20)$$

Finally, spatial modulation (SM) is IM-based modulation technique that codes the information on both TX antenna index and the physical property of molecules such as molecule type [17], concentration level [18] and the release time [19]. With the SM, data rate is increased because by using different types of molecules and TX antenna indices as an information carrier, MSSK and MoSK is combined resulting an increment in the transmitted bits in one symbol. Similarly, MSSK and CSK or MSSK and PPM can be combined to form a SM scheme.

3. SPACE-TIME EQUALIZATION

Space-time equalization is a technique that we propose to the literature and increases the error rate performance of the IM-based MIMO modulation techniques significantly. After absorption of molecules at the RX unit, an equalization operation is performed before MCD. This technique can be applied in only space domain, only time domain or both space and time domain called as space equalization, time equalization and space-time equalization respectively.

3.1 Space Equalization

In MIMO channels, molecules can be received in any RX antennas due to the nature of Brownian motion. After transmission at TX_i, the highest number of molecules will be absorbed by RX_i. Other than RX_i, most arrived molecules will be in the neighboring antennas of RX_i. With a simple equalization operation, number of molecules in the neighboring RX antennas can be taken into calculation in order to regain the transmit power and decrease the ILI effect.

In space equalization, number of molecules at the neighboring antennas of RX_j are multiplied with a coefficient α_{space} and added to the number of molecules at RX_j. In UCA MIMO model, number of molecules after space equalization can be shown as

$$R^{'}_{j-space}[n] = R_j[n] + \alpha_{space}\left(R_{(\hat{j-1})}[n] + R_{(\hat{j+1})}[n]\right), \tag{3.1}$$

where $(\hat{x}) = (x-1)_{n_{RX}} + 1$ and $(.)_{n_{RX}}$ represents the modulo n_{RX} operation. Modulo operation is applied since RX_1 and $RX_{n_{RX}}$ are neighboring antennas to each other in UCA model. After the equalization, MCD can be used for deciding to the data.

The change of BER with respect to α_{space} is shown in Fig. 3.1. In this figure, UCA channel model with parameters $n_{TX} = n_{RX} = 8$, $d_{TX-RX} = 20\mu m$, $r_{UCA} = 15\mu m$ and $r_r = 5\mu m$ is used. Also, bit duration is selected as $t_b = 0.3s$. As it is seen in the figure, the best BER performance is achieved for a positive value of the equalization

19

coefficient, α_{space}. It can be said that, space equalization behaves like increasing transmit power by collecting molecules from neighboring antennas.
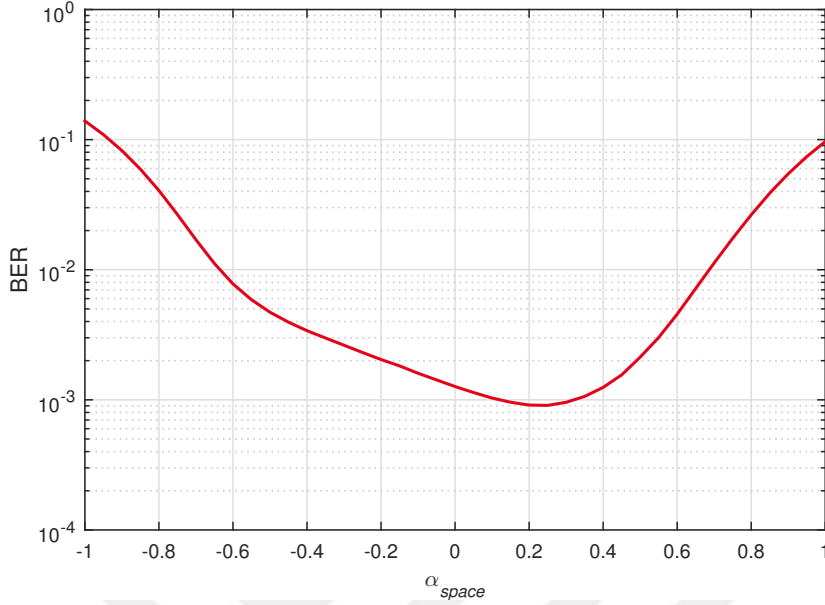
Figure 3.1 : Bit error rate vs. α_{space}.

3.2 Time Equalization

Motion of molecules is random in diffusion environment and after transmission, molecules can reach to the RX antenna at any time. The desired situation is transmitting most of the molecules in the first time slot. Molecules arriving after first time slot causes ISI to the channel and t_s should be selected according to this condition. But if t_s is increased too much, communication speed will be very slow. In order to decrease ISI, an equalization operation is applied by using molecules arrived at the second time slot.

In time equalization, number of molecules arrived in the previous time slot is multiplied with a coefficient α_{time} and added to the current molecule count. After time equalization, the number of molecules is obtained as

$$R'_{j-time}[n] = R_j[n] + \alpha_{time}R_j[n-1]. \tag{3.2}$$

In Fig. 3.2, BER versus α_{time} is presented for the molecular MIMO channel with same parameters in Fig. 3.1. Negative value of the coefficient α_{time} achieves the best BER performance. Since some molecules will arrive late at the RX unit, the purpose of time equalization is to clear the received signal from the ISI effect.

20
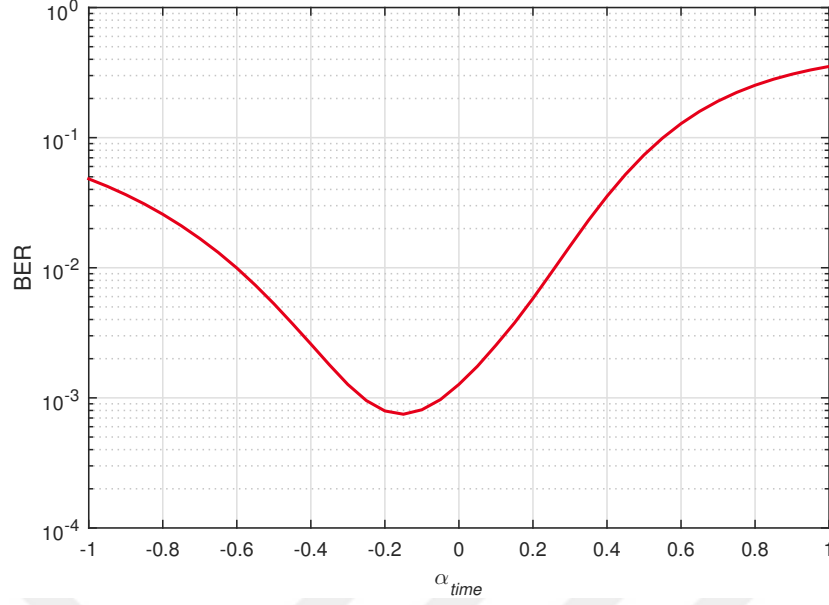
Figure 3.2 : Bit error rate vs. α_{time}.

3.3 Space-Time Equalization

In space-time equalization, both space equalization and time equalization are applied to the system simultaneously in order to unite their powers and come up with a strong technique in terms of error performance. If time equalization is applied to the space equalized system, space-time equalized system will be obtained. Since they are both linear operations, the order of applying time equalization and space equalization does not change the result. Number of molecules after space-time equalization can be derived as

$$R'_{j-spacetime}[n] = R'_{j-space}[n] + \alpha_{time} R'_{j-space}[n-1] \tag{3.3}$$

and by putting (3.1) into (3.3)

$$
\begin{aligned}
R'_{j-spacetime}[n] = R_j[n] + \alpha_{space}\left(R_{(\hat{j-1})}[n] + R_{(\hat{j+1})}[n]\right) + \alpha_{time} R_j[n-1] \\
+ \alpha_{time}\alpha_{space}\left(R_{(\hat{j-1})}[n-1] + R_{(\hat{j+1})}[n-1]\right),
\end{aligned} \tag{3.4}
$$

where $(\hat{x}) = (x-1)_{n_{RX}} + 1$ and modulo n_{RX} operation is denoted as $(.)_{n_{RX}}$. Because of the circular placement in UCA model, modulo operation is applied.

In case of space-time equalization, BER performance with respect to equalization coefficients can be seen in Fig. 3.3. In this figure, same channel parameters with

21

Fig. 3.1 and Fig. 3.2 are used. Based on the simulation, optimum values are calculated as $\alpha_{space} = 0.45$ and $\alpha_{time} = -0.25$. Similar to the individual application of these equalization techniques, the coefficient of space equalization is positive and the coefficient of time equalization is negative. By equalizing in both space and time domains, these techniques empower each other and as a result, space-time equalization becomes very effective in decreasing the error rate.
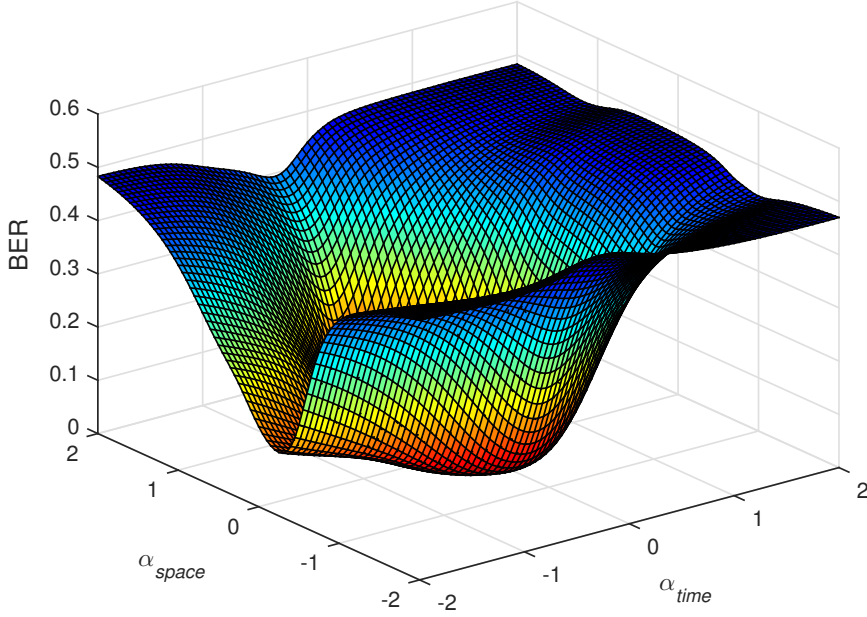
Figure 3.3 : Bit error rate vs. α_{space} and α_{time}.

3.4 Calculation of Time Equalization Coefficients

In this section, an evaluation metric for calculating the optimum time equalization coefficient, α_{time}, is presented. While demodulating the received signal with MCD, finding the antenna index with the maximum arrival count is very critical. In order to separate the intended antenna from the others, we first defined signal to interference difference (SID). SID is calculated by finding the difference between the arrival count of intended antenna and the average arrival count of its neighbors, which have the most arrival count after the intended antenna. *SID* can be shown as

$$SID = \left(\mu_1 - \frac{\mu_2 + \mu_{n_{RX}}}{2} \right), \tag{3.5}$$

where μ_j denotes the expected arrival count in the RX_j.

22

Since MCvD system models have a channel memory, L, there can be $n_{TX}{}^L$ different symbol sequence combinations. A cost function which calculates SID for every symbol combination and returns the minimum SID is defined as

$$f_{cost}(\alpha_{time}) = \min_{\forall x \in [k-L+1;k]} (SID),\qquad (3.6)$$

where $\forall x \in [k-L+1;k]$ represents the every symbol sequence combination. Since time equalization aims to reduce the ISI effect in the system, optimum value of time equalization coefficient can be calculated by finding the value which makes the cost function (3.6) maximum. Optimum value of time equalization coefficient is

$$\alpha_{time-optimum} = \arg\max_{\alpha_{time}} f_{cost}(\alpha_{time}).\qquad (3.7)$$

In this section, the evaluation metric for coefficient of time equalization technique is explained. For space equalization and space-time equalization techniques, we continue to research for developing an evaluation metric.

3.5 Numerical Results

Bit error rate (BER) performances of space equalization, time equalization and space-time equalization are evaluated in this section. Error rate results are obtained with Monte Carlo computer simulations. Firstly, the data is modulated with MSSK modulation scheme at the TX unit and emitted to the UCA MIMO system. At the RX unit, equalization is applied and the resulting signal is demodulated with MCD. Finally, BER is calculated by comparing input and demodulated signals.

We first analyzed equalization techniques in MIMO channel where $n_{TX} = n_{RX} = 4$. Later, these techniques are simulated in a channel model with 8 TX and 8 RX antennas to approve their performance. In both systems, the channel memory is selected as $L = 30$ memory slots and the diffusion coefficient is selected as $D = 79.4\frac{\mu m^2}{s}$.

3.5.1 4x4 MIMO channel

BER performances of equalization techniques are compared with respect to number of emitted molecules, bit duration, radius of RX antenna and distance between TX unit and RX unit.

Simulation parameters are summarized in Table 3.1. Here, M denotes the number of molecules per bit, t_b denotes the bit duration, d_{TX-RX} denotes the distance between TX and RX units, r_r denotes the RX antenna radius and r_{UCA} denotes the radius of UCA. Default parameters for simulations are represented with **boldface** written values in the table.

Table 3.1 : Simulation parameters for space-time equalization technique in 4x4 MIMO system.

Parameter	Value
M (molecules)	$50, 100, \mathbf{150}, 200, 250$
t_b (s)	$0.2, \mathbf{0.3}, 0.4, 0.5, 0.6$
d_{TX-RX} (μm)	$16, \mathbf{18}, 20$
r_r (μm)	$3, 4, \mathbf{5}, 6$
r_{UCA} (μm)	8

Optimum equalization coefficients that used in simulations are obtained with exhaustive search in terms of bit error rate. At the appendix, optimum coefficients are presented in Table A.1, Table A.2, Table A.3 and Table A.4. Note that, $k = \log_2 n_{TX}$ bits per symbol is transmitted in MSSK scheme, symbol duration is $t_s = kt_b$ and the number of molecules per symbol is kM. Also, in 4x4 MIMO channel with UCA formation, TX antennas are separated with $\frac{\pi}{2}$ in angular-wise, so as the RX antennas.

BER performance of both equalization methods with respect to the number of transmitted molecules is presented in Fig. 3.4. Without equalization curve, in which no equalization is applied at the RX unit, is the BER values of MSSK and MCD. With the increasing M, error rates of all curves decreases which is an expected situation for MCvD because M is directly proportional to the mean and the variance of arrival count. Increment in M results in increment in $\frac{\mu_j[k]}{\sigma_j[n]}$ which makes the signal more resistant to the noise. If we compare the equalization methods, space equalization has a very little gain in BER performance for the selected channel parameters and symbol duration because the channel suffers from heavy ISI. In ISI dominated channels, time equalization gives better results than space equalization in terms of BER. By using these two equalization methods together, space-time equalization achieves the best BER performance.

The effect of bit duration t_b on BER performance is demonstrated in Fig. 3.5. In low values of t_b, frequent transmission of molecules results in high ISI and it can be
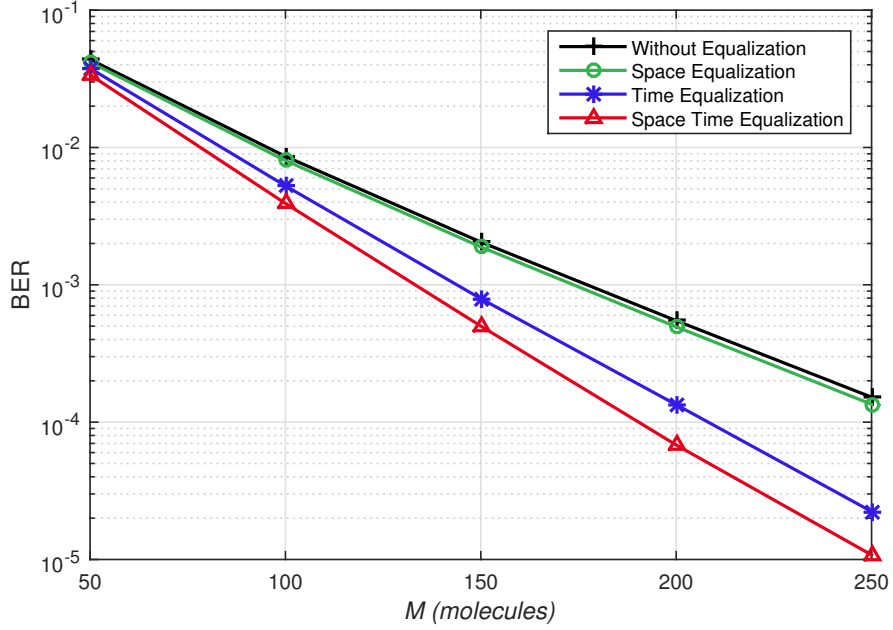
Figure 3.4 : BER vs *M* curves for equalization methods in 4x4 UCA MIMO system.

said that the channel is dominated by ISI. As time equalization targets to decrease ISI effect, it performs well in ISI dominated channels. As the t_b increases, transmissions are scattered in time and the ISI effect is reduced. But this results in ILI dominated channel as the arrival of molecules in the unintended RX antennas increases. In ILI dominated channels, space equalization works better as it regains transmits power by collecting the molecules back from neighboring antennas. Fig. 3.5 clearly shows how space equalization passes the time equalization in BER performance as the channel becomes ILI dominated. Space-time equalization, on the other hand, shows the highest performance for all t_b values because of the simultaneous implementation of space and time equalization.

The effect of distance between TX and RX units can be observed in Fig. 3.6. Default value in our simulations is selected as $d_{TX-RX} = 18 \mu m$. As expected, BER performance for all techniques is degraded with the separation of TX and RX units because molecules begin to arrive later at the RX antennas which results in high ISI. In the channel models with closer TX unit and RX unit, molecules that are emitted from TX unit reach to the RX antennas quicker, resulting reduction in ISI. As d_{TX-RX} decreases, both equalization methods achieve better BER performances while sacrificing from the range of communication.

25
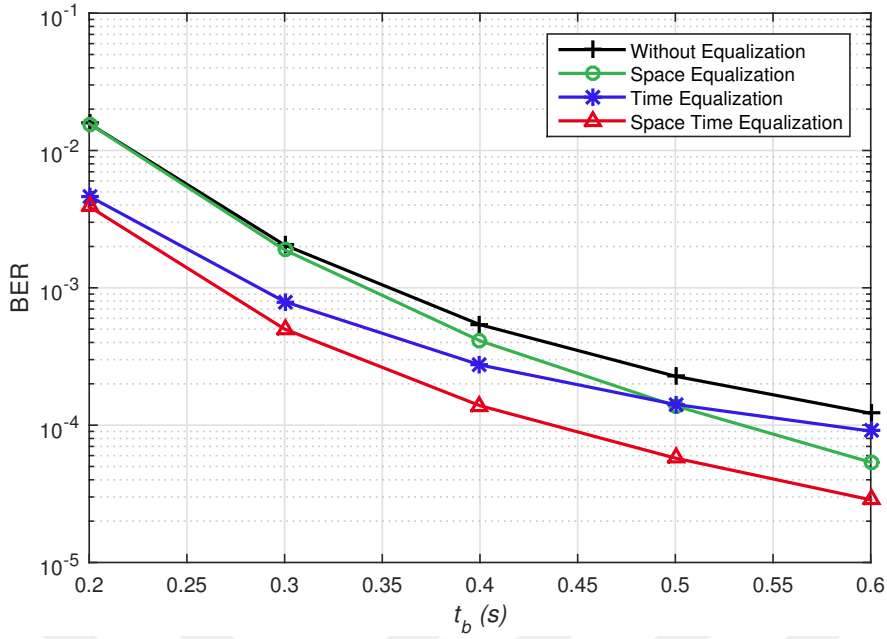
Figure 3.5 : BER vs t_b curves for equalization methods in 4x4 UCA MIMO system.
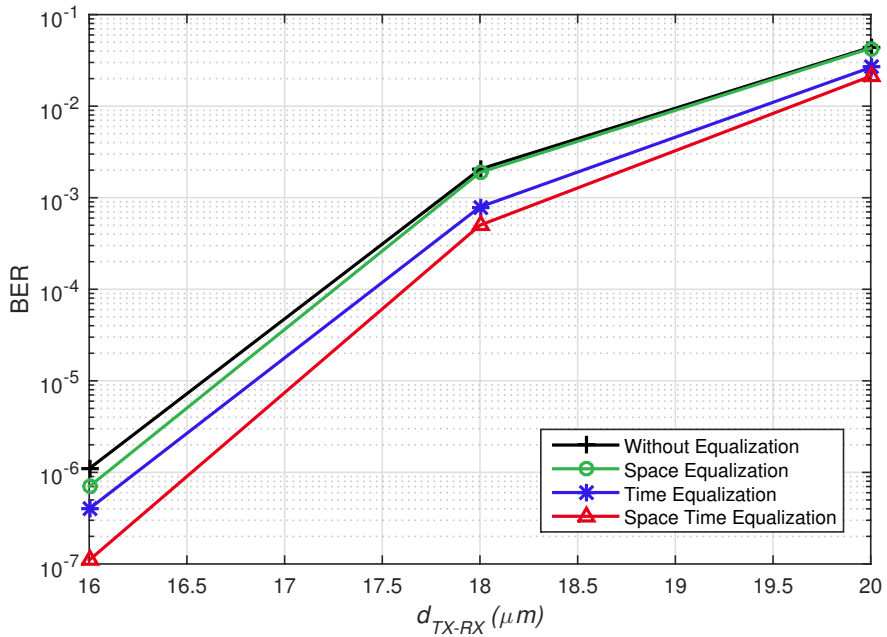
Figure 3.6 : BER vs d_{TX-RX} curves for equalization methods in 4x4 UCA MIMO system.

Fig. 3.7 shows the BER performance of equalization techniques for varying RX antenna radius. As r_r decreases, absorbing area of RX antennas also decreases which results in less arrival at the intended RX antenna. It can be seen in the figure that space equalization performs slightly better than time equalization for $r_r = 3\mu m$. As r_r increases, time equalization outperforms the space equalization. The best BER performance is obtained with space-time equalization as always.
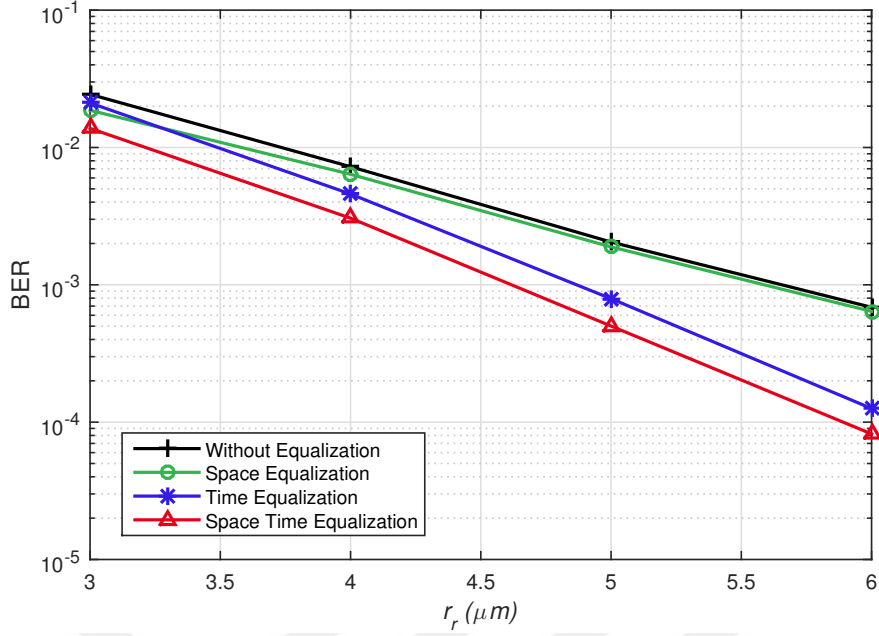
Figure 3.7 : BER vs r_r curves for equalization methods in 4x4 UCA MIMO system.

3.5.2 8x8 MIMO channel

The effect of molecule count, bit duration, separation of antennas and separation of TX and RX unit on the BER performance is examined for equalization techniques in this section. Table 3.2 shows the simulation parameters. Also, optimum values which are obtained by exhaustive search are presented in Table A.5, Table A.6, Table A.7 and Table A.8 at the appendix. In 8x8 MIMO channel, there are 8 TX antennas with $\frac{\pi}{4}$ angular difference between them, same for the RX antennas, as a result of UCA formation.

Table 3.2 : Simulation parameters for space-time equalization technique in 8x8 MIMO system.

Parameter	Value
M (molecules)	$50, 100, \mathbf{150}, 200, 250$
$t_b\ (s)$	$0.15, 0.25, \mathbf{0.35}, 0.45$
$d_{TX-RX}\ (\mu m)$	$18, \mathbf{20}, 22$
$r_{UCA}\ (\mu m)$	$\mathbf{15}, 17.5, 20$
$r_r\ (\mu m)$	5

BER performances of equalization techniques are presented in Fig. 3.8. With the increasing number of molecules, performance improves for both techniques. As explained before, increasing the molecules count results in a higher $\frac{\mu_j[k]}{\sigma_j[n]}$, a more robust

signal against the noise. In this channel, space equalization and time equalization result with close BER gain. It can be said that channel suffers from both ISI and ILI. When space-time equalization is applied, a superior BER performance is obtained. The interesting point in this figure is as M increases, time equalization slightly passes space equalization. Because by increasing number of molecules, transmission power increases and the importance of space equalization decreases when compared with time equalization.
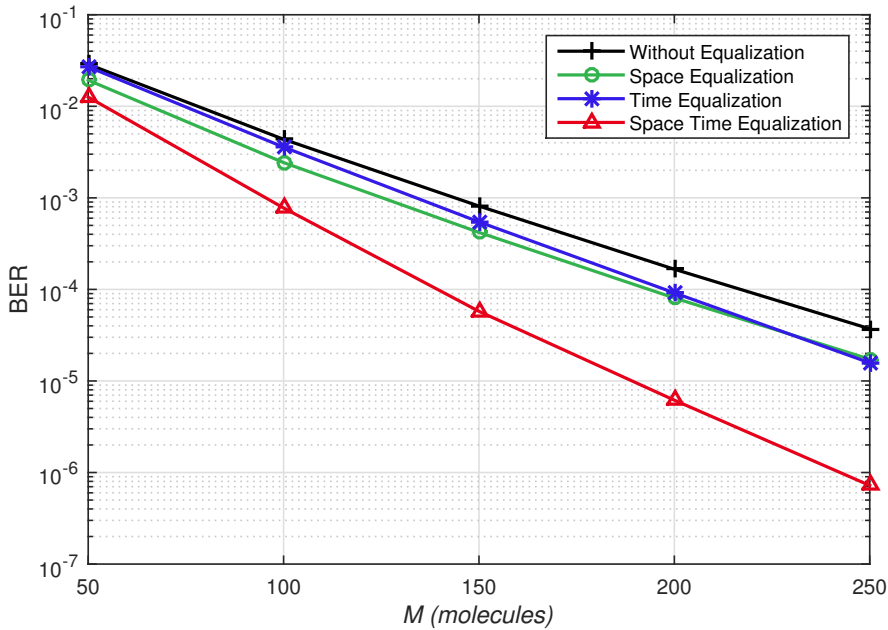
Figure 3.8 : BER vs M curves for equalization methods in 8x8 UCA MIMO system.

The effect of bit duration can be observed in Fig. 3.9. Very similar to the findings in 4x4 MIMO channel, increment in t_b results in ILI dominated channel and space equalization performs better than time equalization. On the other hand, channel is dominated by ISI for the low values of t_b and time equalization has lower error rate than space equalization. As usual, space-time equalization outperforms the other equalization techniques.

BER performance vs. the distance between TX unit and TX unit, which is also similar to the results in 4x4 MIMO channel, is presented in Fig. 3.10. There is a trade-off between the BER performance and the range of communication. Both techniques are affected badly in terms of error rate for increasing d_{TX-RX}. Also, space equalization and time equalization have a close BER performance for the chosen channel parameters. So, it can be concluded that channel is balanced in ISI and ILI.
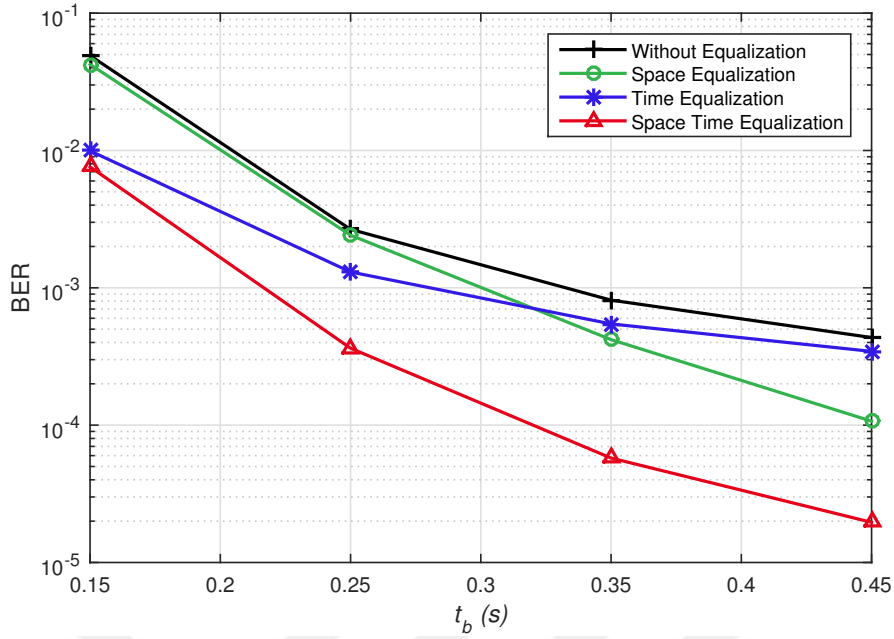
Figure 3.9 : BER vs t_b curves for equalization methods in 8x8 UCA MIMO system.
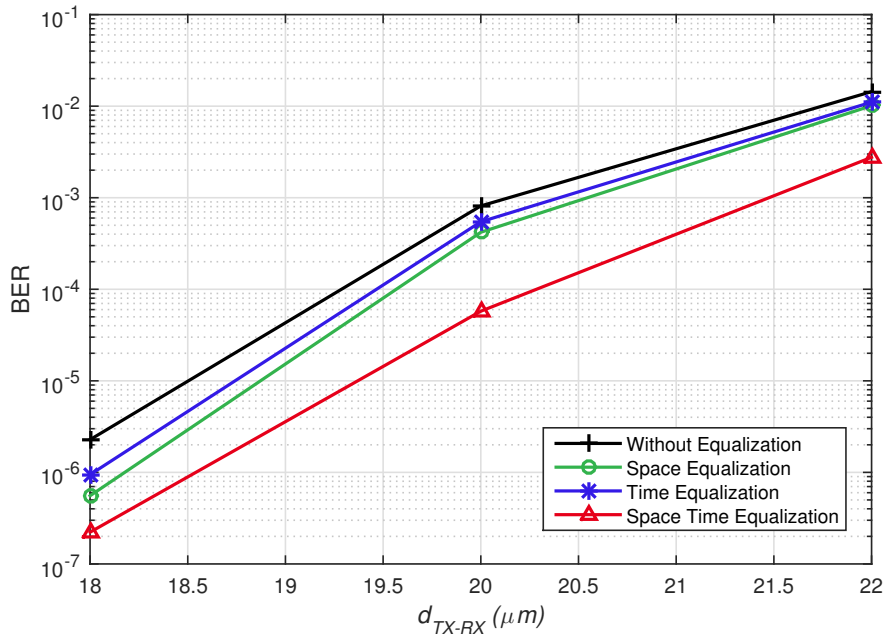
Figure 3.10 : BER vs d_{TX-RX} curves for equalization methods in 8x8 UCA MIMO system.

Fig. 3.11 presents the effect of antenna separation to the BER performance. When RX antennas are closer to each other, more molecules are arrived at the unintended RX antennas which results in ILI dominated channel. For the lower values of r_{UCA}, space equalization have a better BER performance than time equalization. As the radius of UCA increases, RX antennas are separated from each other and ILI decreases. But antenna separation also causes higher ISI because neighboring antennas

29

prevent molecules to arrive in following time slots as RX antennas are absorbing molecules from medium [17]. As a result, time equalization performs better than space equalization in the channels that RX antennas are separated. Independent from the channel is dominated by ISI or ILI, space-time equalization operates best in terms of bit error rate.
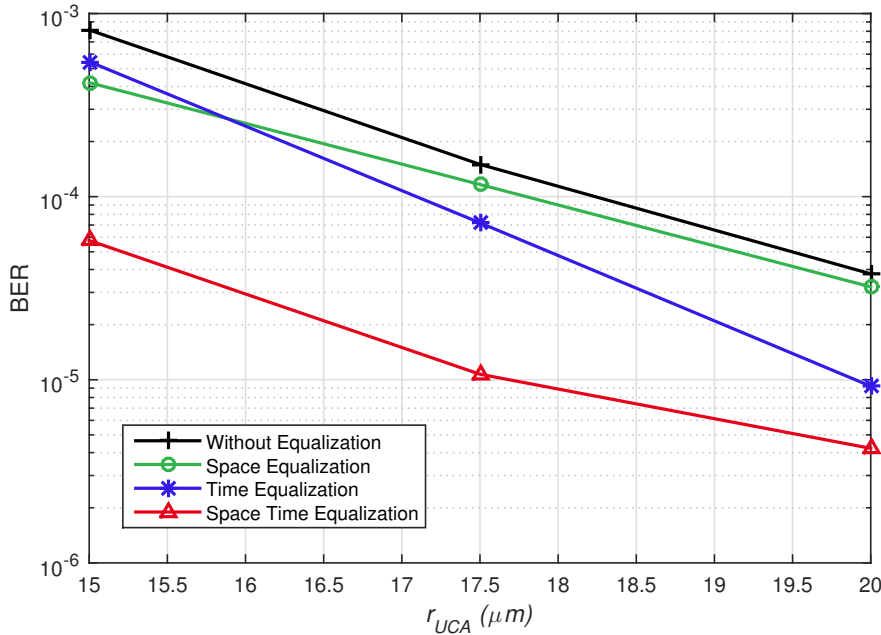
Figure 3.11 : BER vs r_{UCA} curves for equalization methods in 8x8 UCA MIMO system.

3.5.3 Performance of evaluation metric for time equalization

Optimum equalization coefficients in the previous BER simulation are obtained by exhaustive search. In this section, we investigate the performance of evaluation metric that proposed for time equalization and compare it with the coefficients of exhaustive search. For 4x4 UCA MIMO model, default channel distances that presented in 3.1 is used. Under varying bit duration, α_{time} coefficients calculated by exhaustive search and evaluation metric is shown in Table 3.3.

Table 3.3 : Time equalization coefficients (α_{time}) of 4x4 UCA MIMO system.

t_b (s)	Evaluation Metric	Exhaustive Search
0.3	-0.22	-0.17
0.4	-0.15	-0.12
0.5	-0.12	-0.10
0.6	-0.09	-0.06

The performance of evaluation metric is presented in Fig. 3.12. Coefficients obtained from evaluation metric have a very close BER performance to the results of exhaustive search. The advantage of evaluation metric is being much more efficient than exhaustive search in terms of computational cost which makes the evaluation metric a practical method.
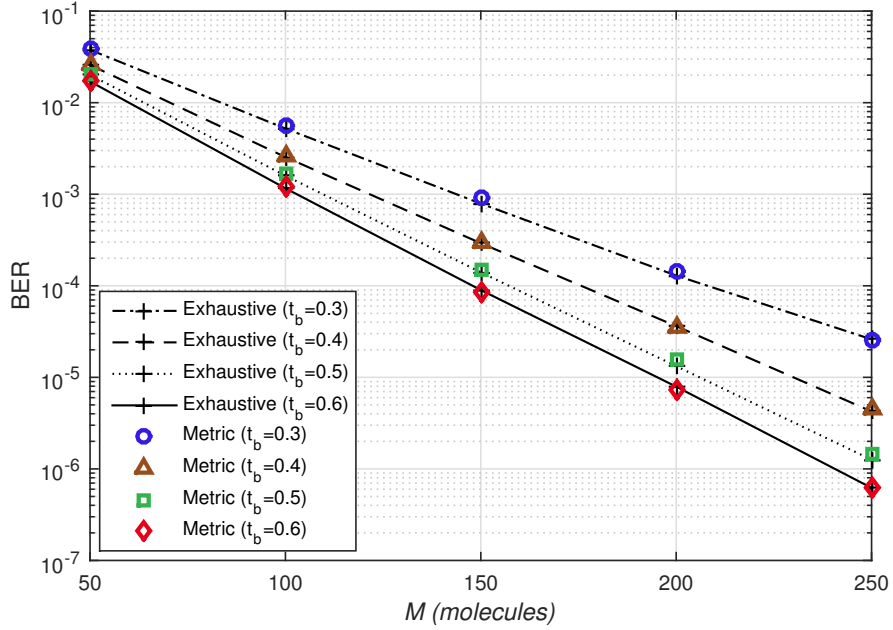
Figure 3.12 : BER performance of evaluation metric in 4x4 UCA MIMO system.

The performance of evaluation metric is repeated in 8x8 UCA MIMO model. Channel distances are selected as the default values in Table 3.2. Calculated α_{time} values by using evaluation metric and exhaustive search are presented in 3.4.

Table 3.4 : Time equalization coefficients (α_{time}) of 8x8 UCA MIMO system.

t_b (s)	Evaluation Metric	Exhaustive Search
0.15	-0.35	-0.39
0.25	-0.20	-0.19
0.35	-0.12	-0.13
0.45	-0.09	-0.08

Fig. 3.13 presents the BER performance of evaluation metric. Error rates of exhaustive search and evaluation metric is almost the same so as the calculated coefficients. By using the proposed evaluation metric, time equalization coefficients can be found in a with a very low computational consumption.
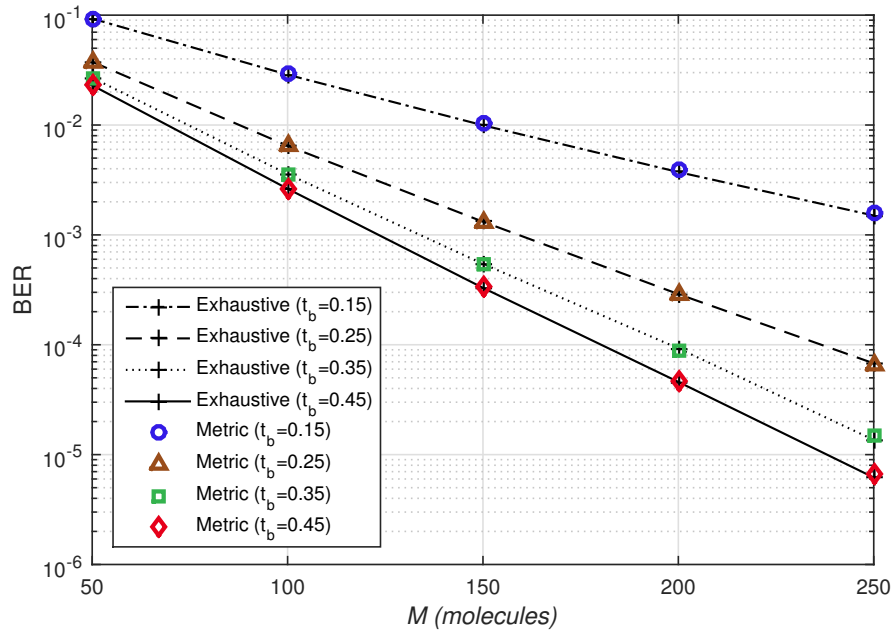
Figure 3.13 : BER performance of evaluation metric in 8x8 UCA MIMO system.

4. A ROBUSTNESS APPROACH FOR ANGULAR MISALIGNMENT

IM-based modulation techniques have great advantages in molecular MIMO channels for increasing data rate and having a better BER performance. At the RX unit, MCD is one of the best options for demodulating the symbol with its low complexity. In the literature, studies assume the perfect alignment of the system for IM-based techniques and MCD among the communication. But in practical scenarios, alignment of the TX unit and RX unit could be lost since system model is in liquid environment. In this section, a robust technique is proposed as a solution for the critical angular misalignment problem without increasing the complexity of the system considerably. This method applies a linear diversity combiner coordinated with the MCD at the RX unit.

4.1 Channel Model for the Misaligned System

The communication system is modeled as a molecular MIMO channel with n_{TX} TX antennas and n_{RX} RX antennas which are placed in a UCA formation. TX antennas are separated from each other with the angle of $\frac{2\pi}{n_{TX}}$. Similarly, the angular difference between RX antennas is $\frac{2\pi}{n_{RX}}$. The parameters d_{TX-RX} and r_{UCA} refer to the same distances as explained for UCA MIMO model in Chapter 2. In addition to that model, angular rotation is also considered in the direction of *yz*-plane which causes angular misalignment. The angular difference between TX unit and RX unit is denoted as θ and we investigate the system for $0 \leq \theta \leq \frac{\pi}{n_{TX}}$ because of the symmetry of UCA model. The overall system model is presented in Fig. 4.1. Note that, the closest distance between the TX antenna and corresponding RX antenna is $d_{TX-RX} - 2r_r$ for only in the perfect alignment case.

In our studies, random-walk based Monte Carlo simulations are used for deriving hitting rate probabilities and channel coefficients, $h_{i,j}[k]$. For each different channel parameters, simulation is run with 10^6 molecules and the time step is selected as
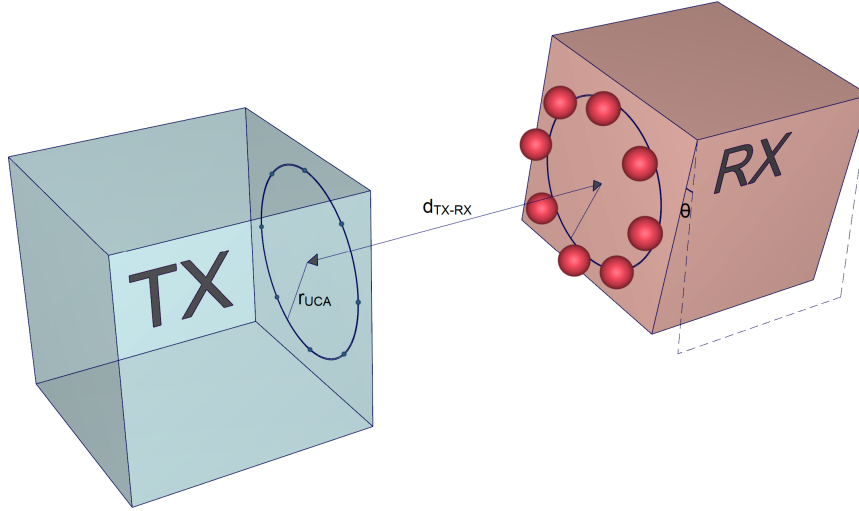
Figure 4.1 : UCA MIMO channel model with angular misalignment.

$\Delta T = 10^{-4} s$. The number of molecules absorbed at RX_j, $R_j[n]$, can be calculated as explained in Chapter 2 with (2.10) and (2.11).

4.2 Proposed Method

MSSK modulation, in which the TX antenna index is an information carrier, is a powerful MIMO technique when used with MCD at the RX. But the misalignment of the system may harshly affect the performance since it is very critical to detect active TX antenna. To overcome this problem, we propose a low complexity approach which applies a linear diversity combiner to the received signal before decoding with the MCD.

Let $R_j[n]$ be the number of molecules absorbed by RX_j at the nth time slot. Arrival vector at n^{th} time slot is denoted by $r[n]$ which can be shown as

$$r[n] = \begin{bmatrix} R_1[n] & R_2[n] & \cdots & R_{n_{RX}}[n] \end{bmatrix}^T. \tag{4.1}$$

After the reception of molecules at RX, the arrival vector is element-wise multiplied with a diversity combining vector and the sum of resulting vector's elements is calculated. This diversity combining operation is repeated for each RX antenna. Number of molecules at RX_j after diversity combining is

$$R_j'[n] = \sum_{k=1}^{n_{RX}} \left(r[n] \circ v_j \right)_k, \tag{4.2}$$

34

where $\circ$ represents the element-wise multiplication and $(.)_k$ represents the kth element of its argument vector. Also, v_j is the diversity combining vector for RX_j.

Knowledge of CIR at the RX unit is essential for misaligned systems in order to generate diversity combining vector. As proposed in [27], maximum likelihood and least squares estimators can be used for deriving CIR by sending training sequences. Under the assumption of estimating the channel coefficients at the Rx unit perfectly, diversity combining vector is heuristically chosen as

$$v_j = \begin{bmatrix} h_{j,1}[1] & h_{j,2}[1] & \cdots & h_{j,n_{RX}}[1] \end{bmatrix}^T. \tag{4.3}$$

Since TX antennas and RX antennas are placed symmetrically on their TX unit and RX unit in UCA modeling, the channel coefficient between TX_1 and RX_j is equal to the channel coefficient between TX_i and RX_{i+j-1} which can be shown as $h_{1,j}[1] = h_{i,i+j-1}[1]$. So, diversity combining vector v_j can be found as

$$v_j = [v_1]_{j-1}, \tag{4.4}$$

where $[.]_{j-1}$ denotes the $j-1^{th}$ cyclic shift of its argument vector. After the diversity combining operation is applied to the arrival vector, data can be demodulated with MCD as

$$\hat{x}[n] = \arg \max_{j \in [1, \cdots, n_{RX}]} R_j^{'}[n]. \tag{4.5}$$

Note that, we evaluated the performance of the diversity combining operation for angular misalignment by using MSSK modulation scheme in the UCA MIMO model. Still, our approach can be adapted for linear MIMO model in which (4.4) is not valid and v_j vectors should be calculated separately. In addition, diversity combining can be applied for any IM-based modulation technique such as SM schemes in which decoding the antenna indices is crucial.

4.3 Numerical Results

In this section, symbol error rate (SER) of the proposed diversity combining technique as a solution for angular misalignment is analyzed and compared with the conventional MCD with Monte Carlo-based computer simulations. At the TX unit, data is modulated with 8-MSSK and emitted to the channel. The system is modeled as 8x8

UCA MIMO model with a possibility of angular misalignment. Diffusion coefficient and the channel memory are selected as $D = 79.4\frac{\mu m^2}{s}$ and $L = 30$ memory slots respectively. In our simulations, we investigated misaligned systems with the angular differences $\theta = \frac{\pi}{32}, \frac{\pi}{24}, \frac{\pi}{16}$ and $\frac{\pi}{8}$. In addition, $\theta = 0$ is considered which is the perfectly aligned system. Since $n_{TX} = n_{RX} = 8$ in our simulation model, TX antennas are angular-wise separated with the angle $\frac{\pi}{4}$. In the angular misalignment where $\theta = \frac{\pi}{8}$, each RX antenna is aligned to the middle of its two neighboring TX antennas which is the most extreme misalignment case. Due to the symmetry of the system model, misalignment angle higher than $\frac{\pi}{8}$ can be represented with a lower value. The equivalence can be shown as $\theta \equiv \theta + i\frac{\pi}{8}$, where i is an integer number.

Table 4.1 displays the simulation parameters where **boldface** written values are default parameters. The effect of number of molecules (M), bit duration (t_b) and the radius of UCA (r_{UCA}) on SER is evaluated for the values in table. Also, SER vs. θ is observed for the diversity combining solution and the conventional MCD.

Table 4.1 : Simulation parameters for the low complexity solution in case of angular misalignment in the system.

Parameter	Value
M (molecules)	$50, 100, \mathbf{150}, 200, 250$
t_b (s)	$0.2, \mathbf{0.3}, 0.4, 0.5$
d_{TX-RX} (μm)	20
r_{UCA} (μm)	$\mathbf{15}, 17.5, 20, 22.5$
r_r (μm)	5

In Fig. 4.2, SER performance of both the conventional MCD and the proposed approach is presented with respect to θ. It is clearly seen that increment of the angular difference between TX unit and RX unit harshly affects the SER performance of the conventional MCD. Since MCD counts the received molecules and decides according to the maximum arrival, perfect alignment of the system is very critical. As θ increases, error rate of conventional MCD also increases. For $\theta = \frac{\pi}{8}$, conventional MCD is unable to demodulate the received signal because each RX antenna is equidistant to the two neighboring TX antennas. However, our proposed approach applies a diversity combining operation by multiplying the arrival count with channel coefficients. With the linear diversity combiner, effect of angular misalignment can be suppressed successfully by weighting the arrival counts. Even for $\theta = \frac{\pi}{8}$, proposed approach outputs an acceptable performance in terms of SER.

Figure 4.2 : SER vs θ curves for proposed approach as a solution of angular misalignment in 8x8 UCA MIMO system.

SER vs. number of transmitted molecules is demonstrated in Fig. 4.3. While M increases, the ratio $\frac{\mu_j[k]}{\sigma_j[n]}$ also increases resulting a transmit power gain. As expected, error rate for both curves decreases with the increment of M. If the figure is examined closely, it can be seen that the curves of proposed approach stands close to each other while gap between the curves of conventional MCD rises with the increasing θ.

Figure 4.3 : SER vs M curves for proposed approach as a solution of angular misalignment in 8x8 UCA MIMO system.

The effect of bit duration on SER performance is shown in the Fig. 4.4. For the lower values of t_b, our proposed approach stays behind the conventional MCD in perfectly aligned channel but protects the system in case of angular misalignment. As t_b increases, proposed approach outperforms the conventional MCD for all channels. Since increasing t_b means more sparse release of molecules, it decreases ISI and results in ILI dominated channel. It can be concluded that the proposed approach can be used for diversity gain in the ILI dominated channels.

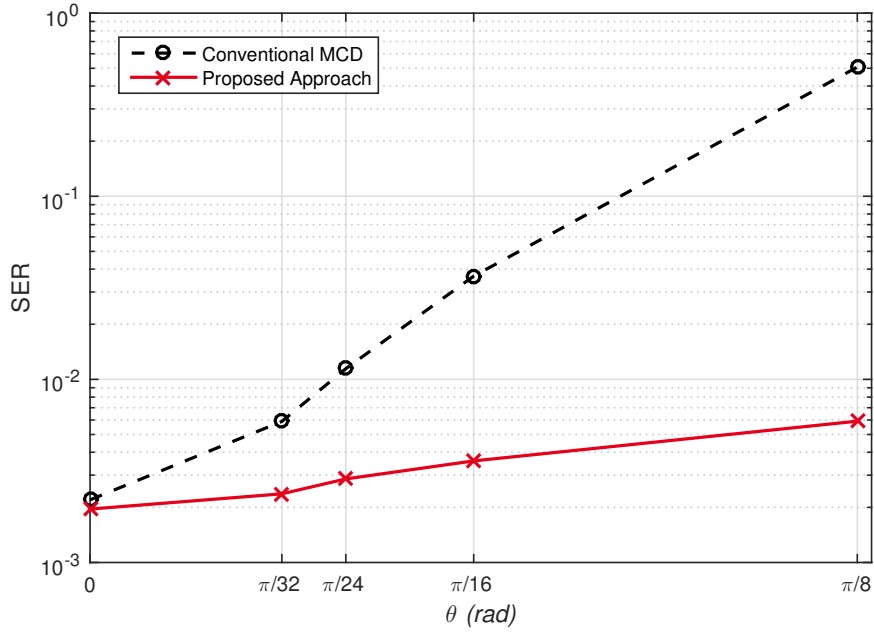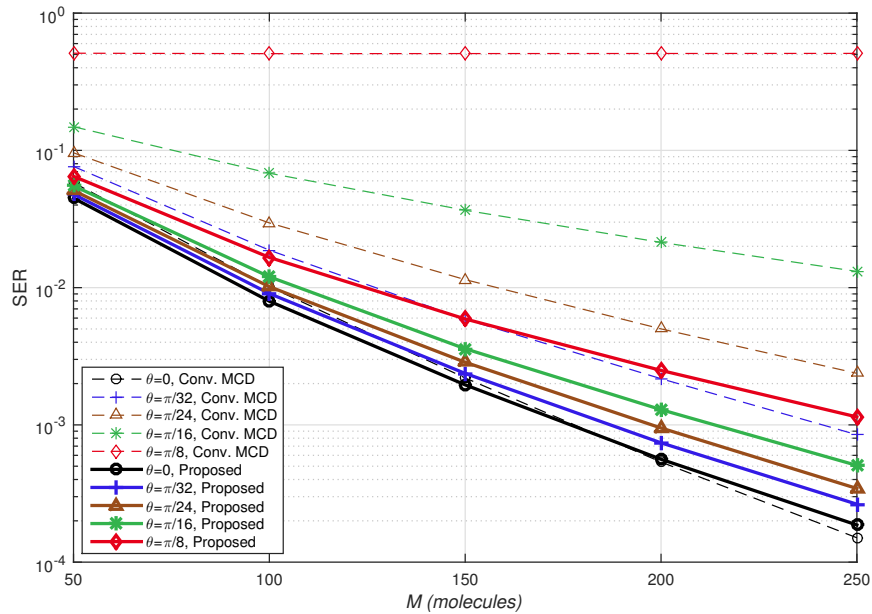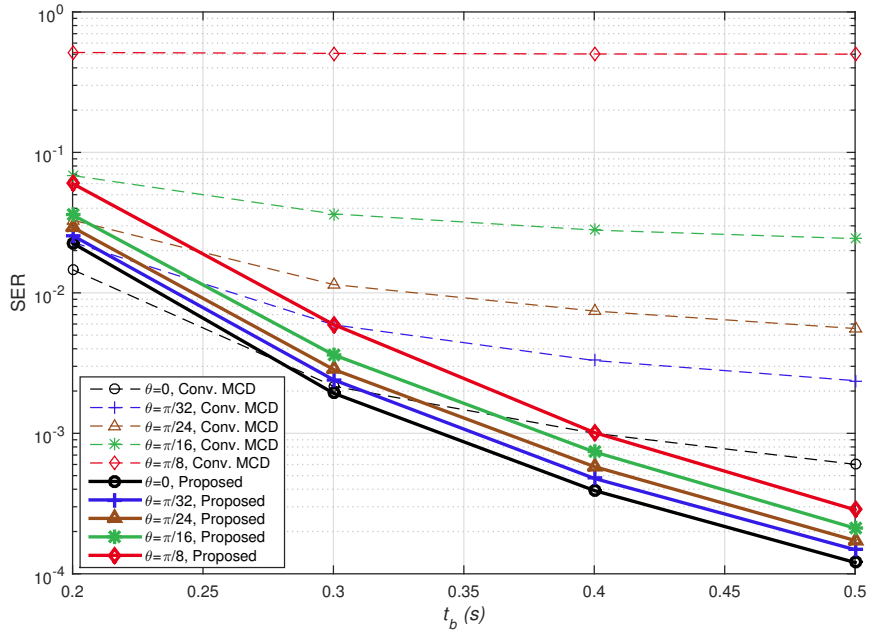**Figure 4.4** : SER vs t_b curves for proposed approach as a solution of angular misalignment in 8x8 UCA MIMO system.

SER performance of conventional MCD and the proposed approach is presented in Fig. 4.5 under the varying r_{UCA}. The increment of r_{UCA} decreases the ILI effect by separating antennas. However, it also increases the ISI because molecules are removed from the environment by absorbing RX antennas and the late arrival of the molecules is prevented. Further separation of antennas reduces this ISI cancellation effect of RX antennas. With the change in r_{UCA}, we face a trade-off between decreasing ISI and decreasing ILI. As it is mentioned before, our proposed diversity combiner works better in ILI dominated channels. Until a certain value of r_{UCA}, separating antennas has a positive impact on SER performance. But after that certain value, channel becomes ISI dominated and error rate starts to increase. There is an optimum r_{UCA} value in each channel for the best SER performance. As r_{UCA} increases, our proposed method

performs worse than the conventional MCD for the perfect alignment case because of the ISI domination. Still, our diversity combining method is essential as a protection for angular misalignment.

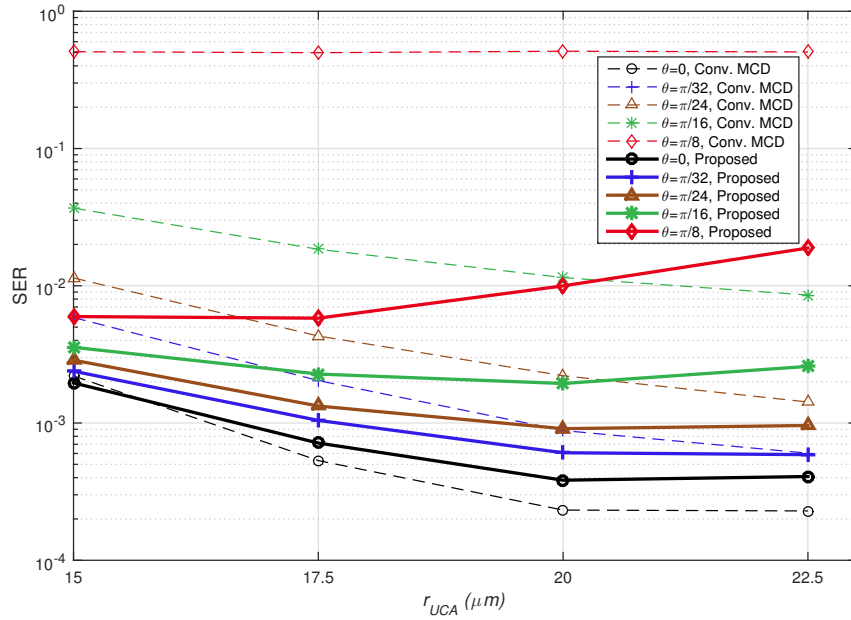**Figure 4.5** : SER vs r_{UCA} curves for proposed approach as a solution of angular misalignment in 8x8 UCA MIMO system.

5. CONCLUSIONS AND RECOMMENDATIONS

In this thesis, we have proposed space-time equalization technique and a low complexity solution for a channel with angular misalignment. Both these two techniques have been applied at RX unit and proposed for IM-based modulation schemes. In molecular MIMO literature, MSSK is a very effective IM-based modulation since it emits molecules as a pulse into the channel and only one antenna is active at a time which makes MSSK resistant to interference. Space-time equalization aims to improve the performance of MSSK ad come up with a strong communication method in terms of error performance. On the other hand, the aim of our diversity combining solution is solving a possible misalignment problem in molecular MIMO channels.

Space-time equalization has been simulated in both 4x4 and 8x8 UCA MIMO channel. It has been discussed that channel may be dominated by ISI or ILI according to the channel parameters and bit duration. Space equalization worked well in ILI dominated channels since it behaves like regaining its transmit power by collecting the molecules from neighboring antennas. However, time equalization performed better than space equalization in ISI dominated channels because it removes the molecules arrived at the second time slot after transmission which represents the serious part of ISI. Finally, space-time equalization resulted as a very promising technique by using attributes of both space equalization and time equalization and improved the error performance significantly. In this thesis, an evaluation metric for easy calculation of time equalization coefficient is presented. By using this metric, time equalization coefficients, which are very close to the optimum values, can be found with computational efficiency. Creating an evaluation metric for space equalization and space-time equalization coefficients has been left a subject of future works.

Our low complexity solution has been evaluated in 8x8 UCA MIMO channel in case of angular misalignment. Even though our technique worsened the error

performance slightly in some systems with the perfect alignment, using diversity combining provided robustness for angular misalignment. As the misalignment angle increases, conventional MCD is affected harshly while our method can still achieve desirable error rates even in the worse case of misalignment. In addition, diversity combiner performed better than conventional MCD in ILI dominated perfectly aligned channel by providing diversity gain and improving error performance. Note that, the diversity combining vector has been heuristically chosen as the channel coefficients at the first time slot in our simulations. Optimum design and calculation of the diversity combining vector is a possible research area in order to achieve better error performance and left as a future work. Also, future work contains simulating misalignment in both three dimensions since we only considered the misalignment in the *yz*-plane.

REFERENCES

[1] **Akyildiz, I.F.**, **Brunetti, F. and Blázquez, C.** (2008). Nanonetworks: A new communication paradigm, *Computer Networks*, *52*(12), 2260–2279.

[2] **Pierobon, M. and Akyildiz, I.F.** (2010). A physical end-to-end model for molecular communication in nanonetworks, *IEEE Journal on Selected Areas in Communications*, *28*(4), 602–611.

[3] **Farsad, N.**, **Yilmaz, H.B.**, **Eckford, A.**, **Chae, C.B. and Guo, W.** (2016). A comprehensive survey of recent advancements in molecular communication, *IEEE Communications Surveys & Tutorials*, *18*(3), 1887–1919.

[4] **Nakano, T.**, **Eckford, A.W. and Haraguchi, T.** (2013). *Molecular communication*, Cambridge University Press.

[5] **Nakano, T.**, **Moore, M.J.**, **Wei, F.**, **Vasilakos, A.V. and Shuai, J.** (2012). Molecular communication and networking: Opportunities and challenges, *IEEE transactions on nanobioscience*, *11*(2), 135–148.

[6] **Moore, M.**, **Enomoto, A.**, **Nakano, T.**, **Egashira, R.**, **Suda, T.**, **Kayasuga, A.**, **Kojima, H.**, **Sakakibara, H. and Oiwa, K.** (2006). A design of a molecular communication system for nanomachines using molecular motors, *Fourth Annual IEEE International Conference on Pervasive Computing and Communications Workshops (PERCOMW'06)*, IEEE, pp.6–pp.

[7] **Tepekule, B.**, **Pusane, A.E.**, **Yilmaz, H.B.**, **Chae, C.B. and Tugcu, T.** (2015). ISI mitigation techniques in molecular communication, *IEEE Transactions on Molecular, Biological and Multi-Scale Communications*, *1*(2), 202–216.

[8] **Kuran, M.S.**, **Yilmaz, H.B.**, **Tugcu, T. and Akyildiz, I.F.** (2011). Modulation techniques for communication via diffusion in nanonetworks, *2011 IEEE international conference on communications (ICC)*, IEEE, pp.1–5.

[9] **Kim, N.R. and Chae, C.B.** (2013). Novel modulation techniques using isomers as messenger molecules for nano communication networks via diffusion, *IEEE Journal on Selected Areas in Communications*, *31*(12), 847–856.

[10] **Kabir, M.H.**, **Islam, S.R. and Kwak, K.S.** (2015). D-MoSK modulation in molecular communications, *IEEE transactions on nanobioscience*, *14*(6), 680–683.

[11] **Garralda, N.**, **Llatser, I.**, **Cabellos-Aparicio, A.**, **Alarcón, E. and Pierobon, M.** (2011). Diffusion-based physical channel identification in molecular nanonetworks, *Nano Communication Networks*, *2*(4), 196–204.

[12] **Meng, L.S.**, **Yeh, P.C.**, **Chen, K.C. and Akyildiz, I.F.** (2012). MIMO communications based on molecular diffusion, *2012 IEEE Global Communications Conference (GLOBECOM)*, IEEE, pp.5380–5385.

[13] **Koo, B.H.**, **Lee, C.**, **Yilmaz, H.B.**, **Farsad, N.**, **Eckford, A. and Chae, C.B.** (2016). Molecular MIMO: From theory to prototype, *IEEE Journal on Selected Areas in Communications*, *34*(3), 600–614.

[14] **Damrath, M.**, **Yilmaz, H.B.**, **Chae, C.B. and Hoeher, P.A.** (2017). Spatial coding techniques for molecular MIMO, *2017 IEEE Information Theory Workshop (ITW)*, IEEE, pp.324–328.

[15] **Basar, E.** (2016). Index modulation techniques for 5G wireless networks, *IEEE Communications Magazine*, *54*(7), 168–175.

[16] **Basar, E.**, **Wen, M.**, **Mesleh, R.**, **Di Renzo, M.**, **Xiao, Y. and Haas, H.** (2017). Index modulation techniques for next-generation wireless networks, *IEEE Access*, *5*, 16693–16746.

[17] **Gursoy, M.C.**, **Basar, E.**, **Pusane, A.E. and Tugcu, T.** (2019). Index modulation for molecular communication via diffusion systems, *IEEE Transactions on Communications*.

[18] **Huang, Y.**, **Wen, M.**, **Yang, L.L.**, **Chae, C.B. and Ji, F.** (2019). Spatial modulation for molecular communication, *IEEE transactions on nanobioscience*.

[19] **Gursoy, M.C.**, **Basar, E.**, **Pusane, A.E. and Tugcu, T.** (2019). Pulse Position-Based Spatial Modulation for Molecular Communications, *IEEE Communications Letters*.

[20] **Yilmaz, H.B.**, **Heren, A.C.**, **Tugcu, T. and Chae, C.B.** (2014). Three-dimensional channel characteristics for molecular communications with an absorbing receiver, *IEEE Communications Letters*, *18*(6), 929–932.

[21] **Damrath, M.**, **Korte, S. and Hoeher, P.A.** (2017). Equivalent discrete-time channel modeling for molecular communication with emphasize on an absorbing receiver, *IEEE transactions on nanobioscience*, *16*(1), 60–68.

[22] **Yilmaz, H.B.**, **Chae, C.B.**, **Tepekule, B. and Pusane, A.E.** (2015). Arrival modeling and error analysis for molecular communication via diffusion with drift, *Proceedings of the Second Annual International Conference on Nanoscale Computing and Communication*, ACM, p. 26.

[23] **Moore, M.J. and Nakano, T.** (2013). Oscillation and synchronization of molecular machines by the diffusion of inhibitory molecules, *IEEE Transactions on Nanotechnology*, *12*(4), 601–608.

[24] **Lee, C.**, **Yilmaz, H.B.**, **Chae, C.B.**, **Farsad, N. and Goldsmith, A.** (2017). Machine learning based channel modeling for molecular MIMO communications, *2017 IEEE 18th International Workshop on Signal Processing Advances in Wireless Communications (SPAWC)*, IEEE, pp.1–5.

[25] **Damrath, M. and Hoeher, P.A.** (2016). Low-complexity adaptive threshold detection for molecular communication, *IEEE transactions on nanobioscience*, *15*(3), 200–208.

[26] **Zare, A.**, **Jamshidi, A. and Keshavarz-Haddad, A.** (2017). Receiver design for pulse position modulation technique in diffusion-based molecular communication, *2017 IEEE 4th International Conference on Knowledge-Based Engineering and Innovation (KBEI)*, IEEE, pp.0729–0733.

[27] **Rouzegar, S.M. and Spagnolini, U.** (2017). Channel estimation for diffusive MIMO molecular communications, *2017 European Conference on Networks and Communications (EuCNC)*, IEEE, pp.1–5.

APPENDICES

APPENDIX A : Optimum Equalization Coefficients

APPENDIX A

Table A.1 : Optimum equalization coefficients used in 4x4 UCA MIMO simulations for default system parameters.

Coefficient	Value
α_{time} (Time)	-0.17
α_{space} (Space)	0.15
α_{time} (Space-time)	-0.20
α_{space} (Space-time)	0.27

Table A.2 : Optimum equalization coefficients used in 4x4 UCA MIMO simulations under varying t_b.

t_b (s)	0.2	0.3	0.4	0.5	0.6
α_{time} (Time)	-0.28	-0.17	-0.12	-0.10	-0.06
α_{space} (Space)	-0.03	0.15	0.23	0.28	0.30
α_{time} (Space-time)	-0.31	-0.20	-0.14	-0.10	-0.08
α_{space} (Space-time)	0.21	0.27	0.32	0.31	0.32

Table A.3 : Optimum equalization coefficients used in 4x4 UCA MIMO simulations under varying d_{TX-RX}.

d_{TX-RX} (μm)	16	18	20
α_{time} (Time)	-0.06	-0.17	-0.26
α_{space} (Space)	0.10	0.15	0.13
α_{time} (Space-time)	-0.11	-0.20	-0.29
α_{space} (Space-time)	0.15	0.27	0.28

Table A.4 : Optimum equalization coefficients used in 4x4 UCA MIMO simulations under varying r_r.

r_r (μm)	3	4	5	6
α_{time} (Time)	-0.13	-0.16	-0.17	-0.20
α_{space} (Space)	0.30	0.21	0.15	0.10
α_{time} (Space-time)	-0.14	-0.18	-0.20	-0.22
α_{space} (Space-time)	0.34	0.29	0.27	0.23

Table A.5 : Optimum equalization coefficients used in 8x8 UCA MIMO simulations for default system parameters.

Coefficient	Value
α_{time} (Time)	-0.13
α_{space} (Space)	0.28
α_{time} (Space-time)	-0.19
α_{space} (Space-time)	0.45

Table A.6 : Optimum equalization coefficients used in 8x8 UCA MIMO simulations under varying t_b.

t_b (s)	0.15	0.25	0.35	0.45
α_{time} (Time)	-0.39	-0.19	-0.13	-0.08
α_{space} (Space)	-0.31	0.13	0.28	0.37
α_{time} (Space-time)	-0.47	-0.28	-0.19	-0.15
α_{space} (Space-time)	0.28	0.39	0.45	0.48

Table A.7 : Optimum equalization coefficients used in 8x8 UCA MIMO simulations under varying d_{TX-RX}.

d_{TX-RX} (μm)	18	20	22
α_{time} (Time)	-0.10	-0.13	-0.18
α_{space} (Space)	0.22	0.28	0.29
α_{time} (Space-time)	-0.16	-0.19	-0.27
α_{space} (Space-time)	0.29	0.45	0.48

Table A.8 : Optimum equalization coefficients used in 8x8 UCA MIMO simulations under varying r_{UCA}.

r_{UCA} (μm)	15	17.5	20
α_{time} (Time)	-0.13	-0.14	-0.17
α_{space} (Space)	0.28	0.17	0.10
α_{time} (Space-time)	-0.19	-0.21	-0.23
α_{space} (Space-time)	0.45	0.42	0.38

CURRICULUM VITAE

Name Surname: Ahmet ÇELİK

Place and Date of Birth: Kadıköy, 10.11.1993

E-Mail: celikahme@itu.edu.tr

EDUCATION:

- **B.Sc.:** 2016, Istanbul Technical University, Faculty of Electrical and Electronic Engineering, Electronics and Communication Engineering Department

PROFESSIONAL EXPERIENCE AND REWARDS:

- 2018-Present Radio Network Planning and Optimization Engineer at Turkcell

PUBLICATIONS, PRESENTATIONS AND PATENTS ON THE THESIS:

- Celik A., Gursoy M. C., Basar E., Pusane A. E., Tugcu T., 2019. A Low-Complexity Solution to Angular Misalignments in Molecular Index Modulation. *IEEE International Symposium on Personal, Indoor and Mobile Radio Communications*, September 8-11, 2019 İstanbul, Turkey.